involved in the first step of the immunopathogenesis of HAM/TSP. In addition, our data strongly suggest that the resistance to apoptotic signals of the peripheral blood $CD4^+$ T cells, including HTLV-I-infected cells of HAM/TSP patients, contributes to the maintenance of long-standing chronic inflammation in the spinal cords of HAM/TSP patients.

However, how activation of Th1 is induced in the peripheral blood HTLV-I-infected cells of HAM/TSP patients? How high HTLV-I proviral load is induced in the peripheral blood of HAM/TSP patients? Although we proposed that activation of the p38 MAPK signaling pathway functions as one of the mechanisms to induce both abnormalities in HAM/TSP patients, the exact mechanisms of how these abnormalities are induced in the peripheral blood of HAM/TSP patients remain unresolved. Since the discovery of HAM/TSP, over 20 years have passed. During that period, numerous findings have been reported in the research field of HAM/TSP [4, 113, 114]. Unfortunately, these findings have not translated into an optimal therapeutic strategy against HAM/TSP. A therapeutic strategy that manages to decrease or delete HTLV-I-infected cells seems to be critical. Therefore, further investigations are needed to clarify the exact mechanisms by which HTLV-I-infected Th1 cells are increased in the peripheral blood of HAM/TSP patients.

Acknowledgements

We are deeply grateful to Dr. Richard Yanagihara, University of Hawai'i at Manoa for his critical review of the manuscript. The summarized studies were supported by a grant from the Neuroimmunological Disease Research Committee, of the Ministry of Health, Labour and Welfare, Japan and by a Grant-in-Aid for Scientific Research from the Ministry of Education, Science, Sports, and Culture of Japan.

References

[1] Yoshida, M. (2001). Multiple viral strategies of HTLV-1 for dysregulation of cell growth control. *Annu. Rev. Immunol, 19,* 475-496.

[2] Osame, M., Usuku, K., Izumo, S., et al. (1986). HTLV-I associated myelopathy, a new clinical entity. *Lancet, i,* 1031-1032.

[3] Jeffery, K.J.M., Usuku, K., Hall, S.E., et al. (1999). HLA alleles determine human T-lymphotropic virus-I (HTLV-I) proviral load and the risk of HTLV-I-associated myelopathy. *Proc. Natl. Acad. Sci. USA, 96,* 3848-3853.

[4] Nakamura, T. (2000). Immunopathogenesis of HTLV-I-associated myelopathy/tropical spastic paraparesis. *Ann. Med, 32,* 600-607.

[5] Osame, M., Matsumoto, M., Usuku, K., et al. (1987). Chronic progressive myelopathy associated with elevated antibodies to human T-lymphotropic virus type I and adult T-cell leukemia-like cells. *Ann. Neurol, 21,* 117-122.

[6] Gessain, A. and Gout, O. (1992). Chronic myelopathy associated with human T-lymphotropic virus type I (HTLV-I). *Ann. Intern. Med, 117,* 933-946.

[7] Höllsberg, P. and Hafler, D.A. (1993). Pathogenesis of diseases induced by human lymphotropic virus type I infection. *N. Engl. J. Med, 328,* 1173-1182.

[8] Akizuki, S., Nakazato, O., Higuchi, Y., et al. (1987). Necropsy findings in HTLV-I associated myelopathy. *Lancet, i,* 156-157.

[9] Iwasaki, Y. (1990). Pathology of chronic myelopathy associated with HTLV-I infection (HAM/TSP). *J. Neurol. Sci, 96,* 103-123.

[10] Umehara, F., Izumo, S., Nakagawa, M., et al. (1993). Immunocytochemical analysis of the cellular infiltrate in the spinal cord lesions in HTLV-I associated myelopathy. *J. Neuropathol. Exp. Neurol, 52,* 424-430.

[11] Umehara, F., Nakamura, A., Izumo, S., et al. (1994). Apoptosis of T lymphocytes in the spinal cord lesions in HTLV-I-associated myelopathy: a possible mechanism to control viral infection in the central nervous system. *J. Neuropathol. Exp. Neurol, 53,* 617-624.

[12] Ijichi, S., Izumo, S., Eiraku, N., et al. (1993). An autoaggressive process against bystander tissues in HTLV-I-infected individuals: a possible pathomechanism of HAM/TSP. *Med. Hypotheses, 41,* 542-547.

[13] Ichinose, K., Nakamura, T., Kawakami, A., et al. (1992). Increased adherence of T cells to human endothelial cells in patients with human T-cell lymphotropic virus type I-associated myelopathy. *Arch. Neurol, 49,* 74-76.

[14] Ichinose, K., Nakamura, T., Nishiura, Y., et al. (1994). Characterization of adherent T cells to human endothelial cells in patients with HTLV-I-associated myelopathy. *J. Neurol. Sci. 122,* 204-209.

[15] Ichinose, K., Nakamura, T., Nishiura, Y., et al. (1996). Characterization of T cells transmigrating through human endothelial cells in patients with HTLV-I-associated myelopathy. *Immunobiol, 196,* 485-490.

[16] Furuya, T., Nakamura, T., Shirabe, S., et al. (1997). Heightened transmigrating activity of CD4-positive T cells through reconstituted basement membrane in patients with human T-lymphotropic virus type I-associated myelopathy. *P. Assoc. Am. Physician, 109,* 228-236.

[17] Sakai, I., Fujii, H., Yoneda, J., et al. (1993). Role of aminopeptidase N (CD13) in tumor-cell invasion and extracellular matrix degradation. *Int. J. Cancer, 54,* 137-143.

[18] Sugita, K., Nojima, Y., Tachibana, K., et al. (1994). Prolonged impairment of very late activating antigen-mediated T cell proliferation via CD3 pathway after T cell-depleted allogeneic bone marrow transplantation. *J. Clin. Invest, 94,* 481-488.

[19] Springer, T.T. (1994). Traffic signals for lymphocyte recirculation and leukocyte emigration: the multiple step paradigm. *Cell, 76,* 301-314.

[20] Bevilacqua, M.P. and Nelson, R.M. (1993). Selectins. *J. Clin. Invest, 91,* 379-387.

[21] Tsujino, A., Nakamura, T., Furuya, T., et al. (1998). Elevated serum levels of soluble E- and L-selectin in patients with human T-cell lymphotropic virus type I-associated myelopathy. *J. Neurol. Sci, 155,* 76-79.

[22] Butcher, E.C. (1991). Leukocyte-endothelial cell recognition: three (or more) steps to specificity and diversity. *Cell, 57,* 1033-1036.

[23] Leeuwenberg, J.F., Smeets, E.F., Neefjes, J.J., et al. (1992). E-selectin and intracellular adhesion molecule-1 are released by activated human endothelial cells in vitro. *Immunology, 77,* 543-549.

[24] Vernant, J.-C., Buisson, G., Magdeleine, J., et al. (1988). T-lymphocyte alveolitis, tropical spastic paraparesis, and Sjögren syndrome. *Lancet, i,* 177.

[25] Sugimoto, M., Nakashima, H., Watanabe, S., et al. (1987). T-lymphotropic alveolitis in HTLV-I-associated myelopathy. *Lancet, ii,* 1220.

[26] Sasaki, K., Morooka, I., Inomata, H., Kashio, N., Akamine, T., Osame, M. (1989). Retinal vasculitis in human T-lymphotropic virus type I associated myelopathy. *Br. J. Ophthalmol, 73,* 812-815.

[27] Nakamura, H., Eguchi, K., Nakamura, T., et al. (1997). High prevalence of Sjögren's syndrome in patients with HTLV-I-associated myelopathy. *Ann. Rheumatic. Dis, 56,* 167-172.

[28] Furuya, T., Nakamura, T., Goto, H., et al. (1998). HTLV-I-associated myelopathy associated with multi-organ inflammatory disease: a case report. *J. Neurol. Sci, 157,* 109-112.

[29] Leppert, D., Waubant, E., Galardy, R., Bunnett, N.W., Hauser, S.L. (1995). T cell gelatinases mediate basement membrane transmigration in vitro. *J. Immunol, 154,* 4379-4389.

[30] Kleiner, D.E. and Stetler-Stevenson, W.G. (1993). Structural biochemistry and activation of metalloproteinases. *Cur. Opin. Cell Biol, 5,* 891-897.

[31] Kambara, C., Nakamura, T., Furuya, T., et al. (1999). Vascular cell adhesion molecule-1-mediated matrix metalloproteinase-2 induction in peripheral blood T cells is up-regulated in patients with HTLV-I-associated myelopathy. *J. Neuroimmunol, 99,* 242-247.

[32] Umehara, F., Izumo, S., Takeya, M., Takahashi, K., Sato, E., Osame, M. (1996). Expression of adhesion molecules and monocyte chemoattractant protein-1 (MCP-1) in the spinal cord lesions in HTLV-I-associated myelopathy. *Acta Neuropathol, 91,* 343-350.

[33] Umehara, F., Okada, Y., Fujimoto, N., Abe, M., Izumo, S., Osame, M. (1998). Expression of matrix metalloproteinases and tissue inhibitors of metalloproteinases in HTLV-I-associated myelopathy. *J. Neuropathol. Exp. Neurol, 57,* 839-849.

[34] Ikegami, M., Umehara, F., Ikegami, N., Maekawa, R., Osame, M. (2002). Selective matrix metalloproteinase inhibitor, N-biphenyl sulfonyl phenylalanine hydroxamic acid, inhibits the migration of $CD4^+$ T lymphocytes in patients with HTLV-I-associated myelopathy. *J. Neuroimmunol, 127,* 134-138.

[35] Itoyama, Y., Kira, J., Fujii, I., Goto, I., Yamamoto, N. (1989). Increases in helper inducer T-cells and activated T-cells in HTLV-I associated myelopathy. *Ann. Neurol, 26,* 257-262.

[36] Jacobson, S., Gupta, T., Mattson, D., Mingioli, E., McFarlin, D.E. (1990). Immunological studies in tropical spastic paraparesis. *Ann. Neurol, 27,* 149-156.

[37] Ries, C. and Petrides, P.E. (1995). Cytokine regulation of matrix metalloproteinase activity and its regulatory dysfunction in disease. *Biol. Chem. Hoppe-Seyler, 376,* 1165-1178.

[38] Sato, H. and Seiki, M. (1993). Regulatory mechanism of 92 kDa type IV collagenase gene expression which is associated with invasiveness of tumor cells. *Oncogene, 8,* 395-405.

[39] Mori, N., Sato, H., Hayashibara, T., et al. (2002). Human T-cell leukemia virus type I tax transactivates the matrix metalloproteinase-9 gene: potential role in mediating adult T-cell leukemia invasiveness. *Blood, 99,* 1341-1349.

[40] Kodama, D., Saito, M., Matsumoto, W., et al. (2004). Longer dinucleotide repeat polymorphism in matrix metalloproteinase-9 (MMP-9) gene promoter which correlates with higher HTLV-I tax mediated transcriptional activity influences the risk of HTLV-I associated myelopathy/tropical spastic paraparesis (HAM/TSP). *J. Neuroimmunol, 156,* 188-194.

[41] Nakajima, M. and Chop, A.M. (1991). Tumor invasion and extracellular matrix degradative enzymes: regulation of activity by organ factors. *Semin. Cancer Biol, 2,* 115-127.

[42] McDonalds, J.K. and Barrett, A.J. (1986). Mammalian proteases. A Glossary and Bibliography, vol. 2: Exopeptidases. London, Academic.

[43] Kunz, D., Bühling, F., Hütter, H.J., et al. (1993). Aminopeptidase N (CD13, EC3.4.11.2) occurs on the surfase of resting and concanavalin A –stimulated lymphocytes. *Biol. Chem. Hoppe Seyler, 374,* 291-296.

[44] Sanderink, G.J., Arthur, Y., Siest, G. (1988). Human aminopeptidases: a review of literature. *J Clin Chem Clin Biochem, 26,* 795-807.

[45] Mosmann,T.R. and Coffman, R.L. (1989). Th1 and Th2 cells: different patterns of lymphokine secretion lead to different functional properties. *Annu. Rev. Immunol, 7,* 145-173.

[46] Seder, R.A. and Paul, W.E. (1994). Acquisition of lymphokine-producing phenotype by CD4$^+$ T-cells. *Annu. Rev. Immunol, 12,* 635-673.

[47] Gubler, U., Chua, A.O., Schoenhaut, D.S., et al. (1991). Co-expression of two distinct genes is required to generate secreted bioactive cytotoxic lymphocyte maturation factor. *Proc. Natl. Acad. Sci. USA, 88,* 4143-4147.

[48] Trinchieri, G. (1995). Interleukin-12: a proinflammatory cytokine with immunoregulatory functions that bridge innate resistance and antigen-specific adaptive immunity. *Annu. Rev. Immunol, 13,* 251-276.

[49] Donckier, V., Abramowicz, D., Bruyns, C., et al. (1994). IFN-γ prevents Th2 cell-mediated pathology after neonatal injection of semi-allogenic spleen cells in mice. *J. Immunol, 153,* 2361-2368.

[50] Racke, M.K., Bnomo, A., Scott, D.E., et al. (1994). Cytokine-induced immune deviation as a therapy for inflammatory autoimmune disease. *J. Exp. Med, 180,* 1961-1966.

[51] Trembleau,S., Penna, G., Bosi, E., Mortara, A., Gately, M.K., Adorini, L. (1995). Interleukin-12 administration induces T helper type 1 cells and accelerates autoimmune diabetes in NOD mice. *J. Exp. Med, 181,* 817-821.

[52] Watanabe, H., Nakamura, T., Nagasato, K., et al. (1995). Exaggerated messenger RNA expression of inflammatory cytokines in human T-cell lymphotropic virus type I-associated myelopathy. *Arch. Neurol, 52,* 276-280.

[53] Nishiura, Y., Nakamura, T., Ichinose, K., et al. (1996). Increased production of inflammatory cytokines in cultured CD4$^+$ cells from patients with HTLV-I-associated myelopathy. *Tohoku. J. Exp. Med, 179,* 227-233.

[54] Furuya, T., Nakamura, T., Fujimoto, T., et al. (1999). Elevated levels of interleukin-12 and interferon-gamma in patients with human T lymphotropic virus type I-associated myelopathy. *J. Neuroimmunol, 95,* 185-189.

[55] Balashov, K., Smith, D., Khoury, S., Hafler, D., Weiner, H. (1997). Increased interleukin-12 production in progressive multiple sclerosis: induction by activated $CD4^+$ T-cells via CD40 ligand. *Proc. Natl. Acad. Sci. USA, 94,* 599-603.

[56] Mosca, P.J., Hobeika, A.C., Clay, T.M., et al. (2000). A subset of human monocyte-derived dendritic cells expresses high levels of interleukin-12 in response to combined CD40 ligand and interferon-gamma treatment. *Blood, 96,* 3499-3504.

[57] Fujimoto, T., Nakamura, T., Nishiura, Y., et al. (2002). Up-regulation of interleukin-12 receptor expression in peripheral blood mononuclear cells of patients with HTLV-I-associated myelopathy/tropical spastic paraparesis. *J. Neurol. Sci, 196,* 21-26.

[58] Murphy, K.M., Ouyang, W., Farrar, J.D., et al. (2000). Signaling and transcription in T helper development. *Annu. Rev. Immunol, 18,* 451-494.

[59] Szabo, S.J., Kim, S.T., Costa, G.L., Zhang, X., Fathman, C.G., Glimcher, L.H. (2000). A novel transcription factor, T-bet, directs Th1 lineage commitment. *Cell, 100,* 655-669.

[60] Zheng, W. and Flavell, R.A. (1997). The transcription factor GATA-3 is necessary and sufficient for Th2 cytokine gene expression in CD4 T cells. *Cell, 89,* 587-596.

[61] Yasukawa, H., Sasaki, A., Yoshimura, A. (2000). Negative regulation of cytokine signaling pathways. *Annu. Rev. Immunol, 18,* 143-164.

[62] Krebs, D.L. and Hilton, D.J. (2001). SOCS proteins: negative regulators of cytokine signaling. *Stem Cells, 19,* 378-387.

[63] Losman, J.A., Chen, X.P., Hilton, D., Rothman, P. (1999). Cutting edge: SOCS-1 is a potent inhibitor of IL-4 signal transduction. *J. Immunol, 162,* 3770-3774.

[64] Alexander, W.S. (2002). Suppressors of cytokine signaling (SOCS) in the immune system. *Nature Rev. Immunol, 2,* 410-416.

[65] Egwuagu, C.E., Yu, C-R., Zhang, M., Mahdi, R.M., Kim, S.J., Gery, I. (2002). Suppressors of cytokine signaling proteins are differentially expressed in Th1 and Th2 cells: implications for Th cell lineage commitment and maintenance. *J. Immunol, 168,* 3181-3187.

[66] Seki, Y., Inoue, H., Nagata, N., et al. (2003). SOCS-3 regulates onset and maintenance of TH2-mediated allergic responses. *Nature Med, 9,* 1047-1054.

[67] Nishiura, Y., Nakamura, T., Fukushima, N., Moriuchi, R., Katamine, S., Eguchi, K. (2004). Increased mRNA expression of Th1-cytokine signaling molecules in patients with HTLV-I-associated myelopathy/tropical spastic paraparesis. *Tohoku J. Exp. Med, 204,* 289-298.

[68] Grogan, J.L. and Locksley, R.M. (2002). T helper cell differentiation: on again, off again. *Curr. Opin. Immunol, 14,* 366-372.

[69] O'Shea, J.J. and Paul, W.E. (2002). Regulation of T_H1 differentiation – controlling the controllers. *Nature Immunol, 3,* 506-508.

[70] Rogge, L., Barberis-Maino, L., Biffi, M., Passini, N., et al. (1997). Selective expression of an interleukin-12 receptor component by human T helper 1 cells. *J. Exp. Med, 185,* 825-831.

[71] Horiuchi, I., Kawano, Y., Yamasaki, K., et al. (2000). Th1 dominance in HAM/TSP and the optico-spinal form of multiple sclerosis versus Th2 dominance in mite antigen-specific IgE myelitis. *J. Neurol. Sci, 172,* 17-24.

[72] Furukawa, Y., Saito, M., Matsumoto, W., et al. (2003). Different cytokine production in Tax-expressing cells between patients with human T cell lymphotropic virus type I (HTLV-I)-associated myelopathy/tropical spastic paraparesis and asymptomatic HTLV-I carriers. *J. Infect. Dis, 187,* 1116-1125.

[73] Nakamura, T., Nishiura, Y., Ichinose, K., et al. (1996). Spontaneous proliferation of and cytokine production by T cells adherent to human endothelial cells in patients with human T-lymphotropic virus type I-associated myelopathy. *Intern. Med, 1996,* 195-199.

[74] Ley, K., Tedder, T. (1995). Leukocyte interactions with vascular endothelium. New insights into selectin-mediated attachment and rolling. *J. Immunol, 155,* 525-528.

[75] Varki, A. (1994). Selectin ligands. *Proc. Natl. Acad. Sci. USA, 91,* 7390-7397.

[76] Austrup, F., Vestweber, D., Borges, E., et al. (1997). P- and E-selectin mediate recruitment of T-helper-1 but not T-helper-2 cells into inflamed tissues. *Nature, 385,* 81-83.

[77] Ohta, S., Hanai, N., Habu, S., Nishimura, T. (1993). Expression of sialyl Lewis^X antigen on human T cells. *Cell Immunol, 151,* 491-497.

[78] Kambara, C., Nakamura, T., Furuya, T., et al. (2002). Increased sialyl Lewis^x antigen-positive cells mediated by HTLV-I infection in peripheral blood CD4$^+$ T lymphocytes in patients with HTLV-I-associated myelopathy. *J. Neuroimmunol, 125,* 179-184.

[79] Hiraiwa, N., Hiraiwa, M., Kannagi, R. (1997). Human T-cell leukemia virus-1 encoded Tax protein transactivates α1 -> 3 fucosyltransferase Fuc-T VII, which synthesizes sialyl Lewis^x, a selectin ligand expressed on adult T-cell leukemia cells. *Biochem. Biophys. Res. Commun, 231,* 183-186.

[80] Natsuka, S., Gersten, K., Zenita, K., Kannagi, R., Lowe, J. (1994). Molecular cloning of a cDNA encoding a novel human leukocyte alpha-1,3-fucosyltransferase capable of synthesizing the sialyl Lewis x determinant. *J. Biol. Chem, 269,* 16789-16794 (published erratum; *J. Biol. Chem, 1994, 269,* 20806).

[81] Ley, K. and Kansas, G.S. (2004). Selectins in T-cell recruitment to non-lymphoid tissues and sites of inflammation. *Nature Rev. Immnol, 4,* 325-335 .

[82] Wagers, A., Waters, C., Stoolman, L., Kansas, G. (1998). Interleukin 12 and interleukin 4 control T cell adhesion to endothelial selectins through opposite effects on α1,3-fucosyltransferase VII gene expression. *J. Exp. Med, 188,* 2225-2231.

[83] Ohmori, K., Takada, A., Ohwaki, I., et al. (1993). A distinct type of sialyl Lewis X antigen defined by a novel monoclonal antibody is selectively expressed on helper memory T cells. *Blood, 82,* 2797-2805.

[84] Yoshie,O., Fujisawa, R., Nakayama, T., et al. (2002). Frequent expression of CCR4 in adult T-cell leukemia and human T-cell leukemia virus type 1-transformed T cells. *Blood, 99,* 1505-1511.

[85] Yoshie, O. (2005). Expression of CCR4 in adult T-cell leukemia. *Leuk. Lymphoma, 46,* 185-190.

[86] Dong, C., Davis, R.J., Flavell, R.A. (2002). MAP kinases in the immune response. *Annu. Rev. Immunol, 20,* 55-72.

[87] Rincón, M. and Pedraza-Alva, G. (2003). JNK and p38 MAP kinases in $CD4^+$ and $CD8^+$ T cells. *Immunol. Rev, 192,* 131-142.

[88] Szabo, S.J., Sullivan, B.M., Peng, S.L., Glimcher, L.H. (2003). Molecular mechanisms regulating TH1 immune responses. *Annu. Rev. Immunol, 21,* 713-758.

[89] Yang, J., Zhu, H., Murphy, T.L., Ouyang, W., Murphy, K.M. (2001). IL-18-stimulated GADD45β required in cytokine-induced, but not TCR-induced, IFN-γ production. *Nature Immunol, 2,* 157-164.

[90] Zhang, S. and Kaplan, M. (2000). The p38 mitogen-activated protein kinase is required for IL-12-induced IFN-γ expression. *J. Immunol, 165,* 1374-1380.

[91] Franklin, A.A., Kubik, M.F., Uittenbogaard, M.N., et al. (1993). Transactivation by the human T-cell leukemia virus tax protein is mediated through enhanced binding of activating transcription factor-2 (ATF-2) ATF-2 response and cAMP element-binding protein (CREB). *J. Biol. Chem, 268,* 21225-21231.

[92] Xu, X., Kang, S.H., Heidenreich, O., Brown, D.A., Nerenberg, M. (1996). Sequence requirements of ATF-2 and CREB binding to the human T-cell leukemia virus type 1 LTR R region. *Virology, 218,* 362-371.

[93] Tan, Y., Rouse, J., Zhang, A., Cariati, S., Cohen, P., Comb, M.J. (1996). FGF and stress regulate CREB and ATF-1 via a pathway involving p38 MAP kinase and MAPKAP kinase-2. *EMBO J, 15,* 4629-4642.

[94] Cuenda, A., Rouse, J., Doza, Y.N., et al. (1995). SB203580 is a specific inhibitor of a MAP kinase homologue which is stimulated by cellular stresses and interleukin-1. *FEBS Lett, 364,* 229-233.

[95] Fukushima, N., Nishiura, Y., Nakamura, T., Yamada, Y., Kohno, S., Eguchi, K. (2005). Involvement of p38 MAPK signaling pathway in IFN-γ and HTLV-I expression in patients with HTLV-I-associated myelopathy/tropical spastic paraparesis. *J. Neuroimmunol, 159,* 196-202.

[96] Nakamura, T., Tsujihata, M., Shirabe, S., Matsuo, H., Ueki, Y., Nagataki, S. (1989). Characterization of HTLV-I in a T-cell line established from a patient with myelopathy. *Arch Neurol, 46,* 35-37.

[97] Yamada, Y., Ohmoto, Y., Hata, T., et al. (1996). Features of the cytokines secreted by adult T cell leukemia (ATL) cells. *Leuk. Lymphoma, 21,* 443-447.

[98] Brown, D.A., Nelson, F.B., Reinherz, E.L., Diamond, D.J. (1991). The human interferon-gamma gene contains an inducible promoter that can be transactivated by tax I and II. *Eur. J. Immunol, 21,* 1879-1885.

[99] Ashkenazi, A. and Dixit, V.M. (1998). Death receptors: signaling and modulation. *Science. 281,* 1305-1312.

[100] Kroemer, G. and Reed, J.C. (2000). Mitochondrial control of cell death. *Nature Med, 6,* 513-519.

[101] Adams, J.M. and Cory, S. (1998). The Bcl-2 protein family: arbiters of cell survival. *Science, 281,* 1322-1326.

[102] Opferman, J.T. and Korsmeyer, S.J. (2003). Apoptosis in the development and maintenance of the immune system. *Nature Immunol, 4,* 410-415.

[103] Green, D. and Reed, J.C. (1998). Mitochondria and apoptosis. *Science, 281,* 1309-1312.

[104] Chen, Q., Gong, B., Almasan, A. (2000). Distinct stages of cytochrome c release from mitochondria: evidence for a feedback amplification loop linking caspase activation to mitochondria dysfunction in genotoxic stress induced apoptosis. *Cell Death Differ, 7,* 227-233.

[105] Hamasaki, S., Nakamura, T., Furuya, T., et al. (2001). Resistance of CD4-positive T lymphocytes to etoposide-induced apoptosis mediated by upregulation of Bcl-xL expression in patients with HTLV-I-associated myelopathy. *J. Neuroimmunol, 117,* 143-148.

[106] Deveraux, Q.L., Roy, N., Steinnicke, H.R., et al. (1998). IAPs block apoptotic events induced by caspase-8 and cytochrome c by direct inhibition of distinct caspases. *EMBO J, 17,* 2215-2223.

[107] Tsukahara, T., Kannagi, M., Ohashi, T., et al. (1999). Induction of Bcl-xL expression by human T-cell leukemia virus type 1 tax through NF-κB in apoptosis-resistant T-cell transfectants with tax. *J. Virol, 73,* 7981-7987.

[108] Baeuerle, P.A. and Henkel, T. (1994). Function and activation of NF-κB in the immune system. *Annu. Rev. Immunol, 12,* 141-179.

[109] Kawakami, A., Nakashima, T., Sakai, H., et al. (1999). Inhibition of caspase cascade by HTLV-I tax through induction of NF-κB nuclear translocation. *Blood. 94,* 3847-3854.

[110] Cheshire, J.L. and Baldwin, A.S. Jr. (1997). Synergistic activation of NF-κB by tumor necrosis factor alpha and gamma interferon via enhanced IκBα degradation and de novo IκBβ degradation. *Mol. Cell Biol, 17,* 6746-6754.

[111] Kishi, S., Saijyo, S., Arai, M., et al. (1997). Resistance to Fas-mediated apoptosis of peripheral T cells in human T lymphocyte virus type I (HTLV-I) transgenic mice with autoimmune arthropathy. *J. Exp. Med, 186,* 57-64.

[112] Arai, M., Kannagi, M., Matsuoka, M., Sato, T., Yamamoto, N., Fujii, M. (1998). Expression of FAP-1 (Fas-associated phosphatase) and resistance to Fas-mediated apoptosis in T cell lines derived from human T cell leukemia virus type 1-associated myelopathy/tropical spastic paraparesis patients. *AIDS Res. Hum. Retroviruses, 14,* 261-267.

[113] Jacobson, S. (2002). Immunopathogenesis of human T cell lymphotropic virus type I-associated neurologic disease. *J. Infect. Dis, 186 (Suppl 2),* S187-192.

[114] Osame, M. (2002). Pathological mechanisms of human T-cell lymphotropic virus type I-associated myelopathy (HAM/TSP). *J. Neurovirol, 8,* 359-364.

MHC Class I-Like MILL Molecules Are β_2-Microglobulin-Associated, GPI-Anchored Glycoproteins That Do Not Require TAP for Cell Surface Expression[1]

Mizuho Kajikawa,*† Tomohisa Baba,‡ Utano Tomaru,‡ Yutaka Watanabe,* Satoru Koganei,§ Sachiyo Tsuji-Kawahara,¶ Naoki Matsumoto,§ Kazuo Yamamoto,§ Masaaki Miyazawa,¶ Katsumi Maenaka,† Akihiro Ishizu,‡‖ and Masanori Kasahara[2]*‡

MILL (MHC class I-like located near the leukocyte receptor complex) is a family of MHC class I-like molecules encoded outside the MHC, which displays the highest sequence similarity to human MICA/B molecules among known class I molecules. In the present study, we show that the two members of the mouse MILL family, MILL1 and MILL2, are GPI-anchored glycoproteins associated with β_2-microglobulin (β_2m) and that cell surface expression of MILL1 or MILL2 does not require functional TAP molecules. MILL1 and MILL2 molecules expressed in bacteria could be refolded in the presence of β_2m, without adding any peptides. Hence, neither MILL1 nor MILL2 is likely to be involved in the presentation of peptides. Immunohistochemical analysis revealed that MILL1 is expressed in a subpopulation of thymic medullary epithelial cells and a restricted region of inner root sheaths in hair follicles. The present study provides additional evidence that MILL is a class I family distinct from MICA/B. *The Journal of Immunology,* **2006, 177: 3108–3115.**

Classical MHC class I molecules, also known as class Ia, are heterodimeric glycoproteins made up of a transmembrane-type H chain and β_2-microglobulin (β_2m).[3] They bind small peptides primarily derived from cytosolic proteins in a groove comprised of the α1 and α2 domains and present them to $CD8^+$ T cells, thereby enabling the immune system to destroy abnormal cells that synthesize viral or other foreign proteins (1). Class Ia molecules are almost ubiquitously expressed and their H chains exhibit an extraordinary level of polymorphism (2).

By contrast, class I molecules, collectively called nonclassical class I or class Ib, are usually oligomorphic or monomorphic, and do not necessarily bind peptides (3–5). Many class Ib molecules have a more restricted tissue distribution than class Ia molecules. Although the majority of class Ib molecules form complexes with β_2m, MICA/B (MHC class I-related chains A and B) (6), zinc-α2-glycoprotein (7), the endothelial protein C receptor (8), and the RAE-1 (retinoic acid early inducible-1) family of class Ib molecules (9) are not associated with β_2m. Furthermore, a significant proportion of class Ib genes (the genes coding for the H chains of class Ib molecules) are located outside the MHC region (5). Accumulated evidence indicates that class Ib molecules have diverse functions ranging from specialized Ag presentation (10–12) to the activation of NK cells (13, 14), transport of IgG (15), pheromone detection (16, 17), and lipid mobilization and catabolism (18).

Recently, we identified a new family of class Ib genes designated *Mill* (MHC class I-like located near the leukocyte receptor complex) in mice (19) and rats (20). The two members of the *Mill* family, *Mill1* and *Mill2*, are located close to the leukocyte receptor complex, thus outside the MHC. *Mill1* and *Mill2* show only limited levels of polymorphism and are transcribed at low levels in most adult tissues. RT-PCR analysis showed that *Mill1* is transcribed in selected tissues such as neonatal thymus and skin whereas *Mill2* is transcribed more ubiquitously at low levels. Predicted MILL1 and MILL2 molecules are glycoproteins with three extracellular domains (α1 to α3), but their α1 and α2 domains lack many of the residues essential for the docking of peptides, suggesting that MILL molecules do not bind peptides. Phylogenetically, MILL1 and MILL2 are most closely related to MICA/B among known class I molecules. Because rodents lack the MICA/B family and conversely, humans do not have the MILL family, we suggested previously that MILL might be a functional substitute for MICA/B (19).

In the present study, we show that MILL1 and MILL2 are GPI-anchored glycoproteins associated with β_2m. Consistent with the absence of critical residues required for the docking of peptides (19), cell surface expression of MILL1 and MILL2 did not require TAP molecules. Immunohistochemical analysis revealed that MILL1 is expressed in a subpopulation of thymic medullary epithelial cells and a restricted region of inner root sheaths in hair follicles. The ability to form complexes with β_2m, anchorage to the membrane by GPI, and unique expression patterns all provide further evidence that MILL is a class I family distinct from MICA/B.

*Department of Biosystems Science, School of Advanced Sciences, Graduate University for Advanced Studies (Sokendai), Hayama, Japan; †Division of Structural Biology, Medical Institute of Bioregulation, Kyushu University, Fukuoka, Japan; ‡Department of Pathology, Hokkaido University Graduate School of Medicine, Sapporo, Japan; §Department of Integrated Biosciences, Graduate School of Frontier Sciences, University of Tokyo, Chiba, Japan; ¶Department of Immunology, Kinki University School of Medicine, Osaka, Japan; and ‖Department of Medical Technology, Hokkaido University School of Medicine, Sapporo, Japan

Received for publication July 26, 2005. Accepted for publication June 16, 2006.

The costs of publication of this article were defrayed in part by the payment of page charges. This article must therefore be hereby marked *advertisement* in accordance with 18 U.S.C. Section 1734 solely to indicate this fact.

[1] This work was supported by grants-in-aid for Scientific Research from the Ministry of Education, Culture, Sports, Science and Technology of Japan, Uehara Memorial Foundation, the Naito Foundation, and the Takeda Science Foundation.

[2] Address correspondence and reprint requests to Dr. Masanori Kasahara, Department of Pathology, Hokkaido University Graduate School of Medicine, North-15, West-7, Sapporo 060-8638, Japan. E-mail address: mkasaha@med.hokudai.ac.jp

[3] Abbreviations used in this paper: β_2m, β_2-microglobulin; MILL, MHC class I-like located near the leukocyte receptor complex; PI-PLC, phosphatidylinositol-specific phospholipase C; PNGase F, peptide:*N*-glycosidase F.

0022-1767/06/$02.00

Materials and Methods

Cell lines and Abs

The mouse T lymphoma cell line RMA ($H2^b$-positive) and its TAP2-deficient mutant RMA-S ($H2^b$-negative) (21) were obtained from Dr. Kärre (Karolinska Institute, Stockholm, Sweden). Cells were maintained in RPMI 1640 medium (Invitrogen) supplemented with 10% (v/v) heat-inactivated FBS at 37°C and 5% CO_2.

Anti-FLAG mAb M2 (F3165) was purchased from Sigma-Aldrich. Goat polyclonal Ab to mouse β_2m (sc-8361) was purchased from Santa Cruz Biotechnology. Anti-human pan-cytokeratin mAb AE1/AE3 (M1590) and anti-human hair shaft cytokeratin mAb AE13 (ab16113) were purchased from DakoCytomation and Abcam, respectively. Mouse anti-H2-K^b mAb (clone AF6–88.5) and anti-CD45 mAb (clone 30-F11) were from BD Pharmingen. The Abs used as secondary reagents were as follows: FITC-labeled goat anti-mouse IgG, $F(ab')_2$ fragment (IM0819; Beckman Coulter), FITC-labeled swine anti-rabbit Ig, $F(ab')_2$ fragment (F0054; DakoCytomation), HRP-conjugated sheep anti-mouse IgG (NA931; Amersham Biosciences), HRP-conjugated donkey anti-rabbit IgG (NA934; Amersham Biosciences), HRP-conjugated donkey anti-goat IgG (sc-2056; Santa Cruz Biotechnology), Alexa Fluor 594-conjugated goat anti-rabbit IgG (A11072; Molecular Probes), and Alexa Fluor 488-conjugated goat anti-mouse IgG (A11001; Molecular Probes). Isotype-matched mouse IgG1 Ab (PP100) and pooled normal rabbit serum (CL1000) were purchased from Chemicon International Inc. and Cedarlane Laboratory Ltd., respectively.

Production of polyclonal Ab against mouse MILL molecules

The α1-α3 domains of MILL1 and MILL2 with 6 × His tags at their N termini were expressed in *Escherichia coli* strain M15 using the pQE30 expression vector following the instructions of the manufacturer (Qiagen). Briefly, the DNA fragments encoding the α1-α3 domains of mouse MILL molecules were amplified by PCR using the BALB/c-derived *Mill* plasmid cDNA (19) as templates. The primer sequences were 5′-TTGCGAGCTC CACACTCTGCGCTATGACCT-3′ (with a *Sac*I site at its 5′-end) and 5′-CCCAAGCTTATATTGTGGTTGCCGTGCTT-3′ (with a *Hin*dIII site at its 5′-end) for MILL1 and 5′-GTGGATCCACCCACACTCTGCGC TATAA-3′ (with a *Bam*HI site at its 5′-end) and 5′-CCCAAGCTTCATC CTGACTGTCCTCAGCA-3′ (with a *Hin*dIII site at its 5′-end) for MILL2. PCR products digested with *Sac*I/*Hin*dIII for MILL1 and *Bam*HI/*Hin*dIII for MILL2 were ligated into *Sac*I/*Hin*dIII- and *Bam*HI/*Hin*dIII-digested pQE30, respectively. After transformation into M15, recombinant proteins were induced by adding isopropyl-1-thio-β-D-galactopyranoside to a final concentration of 1 mM. *E. coli* cells were harvested and lysed in buffer B (100 mM NaH_2PO_4, 10 mM Tris-HCl, 6 M guanidine hydrochloride, pH 8.0), and lysates were centrifuged at 10,000 × *g* for 20 min at room temperature. Ni-NTA acid resins were added to supernatants and mixed gently by shaking. Resin-lysate mixtures were loaded into an empty column and washed twice with buffer C (100 mM NaH_2PO_4, 10 mM Tris-HCl, 6 M guanidine hydrochloride, pH 5.9). Recombinant proteins were eluted by buffer D (100 mM NaH_2PO_4, 10 mM Tris-HCl, 6 M guanidine hydrochloride, pH 4.5), separated by preparative SDS-PAGE, eluted and concentrated. Purified recombinant proteins (200 μg per rabbit) were mixed with CFA and injected into rabbits. After 2, 4, and 6 wk, the animals were boosted with the same amount of recombinant proteins mixed with IFA. Whole bloods were collected and antisera prepared 1 wk after the last boost.

Construction of mammalian expression plasmids

Mouse MILL molecules have an insertion of amino acids between the leader peptide and the α1 domain (19). The coding regions of mouse MILL1 and MILL2 excluding this inserted sequence and the leader peptide were obtained by PCR using the *Mill* plasmid cDNA (19) as templates. The primer sequences were 5′-CCAAGCTTGAACCCCACACTCTGCGC TA-3′ (with a *Hin*dIII site at its 5′-end) and 5′-GTGGATCCCTACCAA CACTGTAGAAAAGAGC-3′ (with a *Bam*HI site at its 5′-end) for MILL1 and 5′-CCAAGCTTACCCACACTCTGCGCTATAA-3′ (with a *Hin*dIII site at its 5′-end) and 5′-GTGGATCCTCAGTTGGCTCTGGCCAGTG-3′ (with a *Bam*HI site at its 5′-end) for MILL2. After digestion with *Hin*dIII/*Bam*HI, the PCR products were ligated to the *Hin*dIII/*Bam*HI-digested pFLAG-CMV-3 expression vector carrying a preprotrypsin leader sequence (Sigma-Aldrich). These constructs, designated MILL1-pFLAG-CMV-3 and MILL2-pFLAG-CMV-3, respectively, enabled the expression of MILL molecules with an N-terminal FLAG tag. In all cases, the integrity of expression constructs was verified by sequencing. DNA for transfection was isolated with the plasmid purification kit purchased from Qiagen.

Establishment of stable transfectants

To establish stable cell lines expressing MILL molecules, RMA and RMA-S cells were transfected with linearized MILL1-pFLAG-CMV-3 or MILL2-pFLAG-CMV-3 plasmids by electroporation at 250 V, 950 μF with Gene Pulser II according to the instructions of the manufacturer (Bio-Rad). Neomycin-resistant cells were selected by treatment with G418 (600 and 800 μg/ml for RMA and RMA-S, respectively) and clones exhibiting high levels of MILL expression were expanded; expression of MILL proteins was monitored by flow cytometry and immunoblotting with anti-FLAG and anti-MILL Abs.

Flow cytometric analysis

For cell surface staining, single cell suspensions (1 × 10^6 cells) were washed with ice-cold PBS (pH 7.4) and incubated in 100 μl of PBS (pH 7.4) containing 0.1% NaN_3 with 1 μg of mAb or isotype controls for 30 min on ice. After washing with ice-cold PBS (pH 7.4), cells were incubated in 100 μl of PBS (pH 7.4) containing 0.1% NaN_3 with the FITC-conjugated F(ab′) fragment of goat anti-mouse IgG or $F(ab')_2$ fragment of swine anti-rabbit Ig (1:200 dilution). Subsequently, cells were washed with ice-cold PBS (pH 7.4) and analyzed by EPICS ALTRA (Beckman Coulter). Data were analyzed with EXPO32 software (Beckman Coulter).

Immunoprecipitation and glycosidase digestion

For purification of FLAG-tagged MILL proteins, RMA-MILL1 and RMA-MILL2 stable transfectants (1 × 10^8 cells) were solubilized by 1 ml of ice-cold lysis buffer (50 mM Tris-HCl, 1 mM EDTA, 150 mM NaCl, 1% Triton X-100, 0.2 mM 4-(2-aminoethyl)-benzenesulfonyl fluoride, 20 μM leupeptin, 1 μM pepstatin, pH 7.5). After incubation for 30 min at 4°C, cell lysates were centrifuged at 13,000 × *g* for 10 min at 4°C to remove cell nuclei and insoluble proteins. Cleared lysates were incubated with protein G-Sepharose beads (Amersham Biosciences) at 4°C for 1 h. Supernatants were incubated with anti-FLAG mAb-coupled protein G-Sepharose beads at 4°C for 1 h. After washing 4 times with lysis buffer, immunoprecipitated proteins were eluted by 0.1 M glycine-HCl (pH 3.0), and immediately neutralized by adding 0.1 M Tris-HCl (pH 9.0). Eluted proteins were denatured and treated with 500 U/μl peptide:*N*-glycosidase F (PNGase F; New England Biolabs) at 37°C for 18 h.

Immunoblotting

To detect MILL proteins and β_2m, samples were incubated in 1 × SDS sample buffer at 95°C for 10 min. Denatured proteins were separated on 12% SDS-PAGE and transferred to Hybond-P polyvinylidene difluoride membranes (Amersham Biosciences) using a semidry blotter (Bio-Rad) at 15 V for 45 min. The blotted membranes were incubated with 5% skim milk or 3% BSA in PBS (pH 7.4) containing 0.1% Tween 20 (PBST) at room temperature for 60 min and then incubated with 1/500 diluted antisera or 1 μg/ml of Ab in PBST at room temperature for 60 min. After washing twice with PBST, the membranes were incubated with 1/25,000 diluted HRP-conjugated anti-mouse, rabbit or goat IgG Abs. After washing three times with PBST, positive bands were visualized using the ECL-Plus (Amersham Biosciences) or the Super Signal West Dura detection system (Pierce).

Phosphatidylinositol-specific phospholipase C (PI-PLC) treatment

RMA-MILL and RMA-S-MILL cells were washed with PBS (pH 7.4) and treated with 1 U/ml PI-PLC (Sigma-Aldrich) in PBS (pH 7.4) at 37°C for 1 h. Subsequently, cells were washed with ice-cold PBS (pH 7.4) and used for flow cytometric analysis.

Coimmunoprecipitation of cell surface MILL molecules

Cell surface MILL proteins expressed on the RMA-MILL stable transfectants were purified by PI-PLC treatment and immunoprecipitation with anti-FLAG Ab-coupled protein G-Sepharose beads. Immunoprecipitates were subjected to immunoblotting using anti-FLAG and anti-mouse β_2m Ab.

Refolding of bacterially expressed MILL ectodomains

cDNA encoding the ectodomains of MILL1 and MILL2 were amplified by PCR using the *Mill* plasmid cDNA (19) as templates. Primers used were 5′-CATTAATGGACAACCAAAGACTGGTG-3′ (sense) and 5′-TCC CCCGGGGGCAGCAGGTTCATTGATA-3′ (antisense) for MILL1, and 5′-CCATATGTCCAGCATCCAAGGAACC-3′ (sense) and 5′-AAAAG TACTGACAGCTGTCTGCATGATG-3′ (antisense) for MILL2. These

primers contained *AseI*, *SmaI*, *NdeI*, or *ScaI* restriction enzyme sites indicated by underlines. The PCR-generated cDNA fragments of MILL1 and MILL2 were cloned into the bacterial expression vector pET3cN-bio, which was designed to express a recombinant protein with an N-terminal enzymatic biotinylation signal (22), to construct MILL1-pET3cNbio and MILL2-pET3cNbio, respectively. Rosetta (DE3) strain of *E. coli* (Novagen, Merck) was transformed with MILL1-pET3cNbio or MILL2-pET3cNbio. Expression of soluble MILL1 or MILL2 was induced with 1 mM isopropyl-1-thio-β-D-galactopyranoside, and MILL proteins were refolded from the purified inclusion bodies by dilution as described previously (22). To examine effects of β_2m on refolding, C57BL/6-derived β_2m (β_2m^b), similarly expressed in *E. coli*, was included in the refolding mixture at the molar ratio of 1:2 (MILL/β_2m). Refolded soluble MILL1 and MILL2 proteins were purified by anion-exchange column chromatography and gel-filtration chromatography. In anion-exchange chromatography on a UNO Q-6 column using 20 mM Tris-HCl buffer (pH 8.5) as a mobile phase, soluble MILL1 or MILL2 refolded in the presence of β_2m was eluted in the approximately 250 mM Cl^- fraction by a 0–500 mM NaCl gradient. The gel-filtration column chromatography was performed on a Superdex 75 10/30 column (Amersham Biosciences) equilibrated with 25 mM Tris-HCl buffer (pH 8.0) containing 150 mM NaCl at the flow rate of 0.5 ml/min. The column was calibrated with gel-filtration standards from Bio-Rad.

Immunohistochemistry

For immunostaining, frozen sections prepared from 3-day-old, 10-day-old, and 6-wk-old male BALB/c mice were fixed using cold acetone for 5 min, washed with PBS, stained by the standard method (23), and then mounted in fluorescent mounting medium (DakoCytomation). Immunofluorescence was detected using a fluorescence microscope (ECLIPSE E600; Nikon). To evaluate the specificity of staining, the antiserum against MILL1 was diluted 1/40 with PBS to a final volume of 1 ml and absorbed with 5×10^7 RMA-MILL1 or RMA cells at 4°C overnight. The preabsorbed antiserum was diluted 1/80 with PBS and used for immunostaining. All experiments using animals have been reviewed and approved by the institutional review committee of Hokkaido University Graduate School of Medicine.

Isolation of thymic stromal cells

Thymi were dissected from 4-wk-old C57BL/6 and β_2m-deficient mice. Breeding pairs of the β_2m-deficient strain, B6.129P2-*B2m*^{tm1Unc}/J (stock no. 002087), were purchased from The Jackson Laboratory, and their progenies were produced at Kinki University School of Medicine. Thymic stromal cells were enriched as described (24). Briefly, thymic fragments were digested in RPMI 1640 medium containing collagenase D and DNase I (both obtained from Roche) at 37°C for 15 min. After repeating this procedure 3 times, cells were pooled and stained with mAb for CD45. CD45-negative fractions containing stromal cells including thymic epithelial cells were subjected to flow cytometric analysis.

Results

Establishment of stable cell lines expressing N-terminally FLAG-tagged MILL molecules and generation of rabbit antisera specific for MILL molecules

To facilitate biochemical analysis, we transfected FLAG-tagged expression plasmids into the mouse T lymphoma cell line RMA and established stable cell lines, RMA-MILL1 and RMA-MILL2, expressing N-terminally FLAG-tagged MILL1 and MILL2 molecules, respectively (Fig. 1*A*). Cell surface expression of MILL1 and MILL2 was confirmed by flow cytometry using the anti-FLAG Ab as well as the rabbit antisera generated against bacterially expressed MILL1 and MILL2 molecules. The specificity of our rabbit antisera was further confirmed by Western blot analysis of whole cell lysates (Fig. 1*B*). The anti-FLAG Ab detected two major bands of 48 and 41 kDa in RMA-MILL1 cells. The band of 41 kDa was nonspecific because it was detected in untransfected RMA cells. A major band of 48 kDa and a minor band of 44 kDa were detected by the anti-MILL1, but not anti-MILL2, antiserum (Fig. 1*B*). In RMA-MILL2 lysates, the anti-FLAG Ab detected bands of 43 and 41 kDa (Fig. 1*B*, *top*), which were also detected with the anti-MILL2, but not anti-MILL1, antiserum (Fig. 1*B*, *bottom*). Thus, the band of 41 kDa detected by the anti-FLAG Ab in RMA-MILL2 cells presumably represents doublets containing both specific and nonspecific signals. We also expressed MILL1 and MILL2 molecules on RMA cells using their endogenous signal peptides and performed cytometric analysis using the MILL-specific rabbit antisera. We obtained staining patterns similar to those shown in Fig. 1*A* (data not shown).

Deduced MILL1 and MILL2 molecules have three potential *N*-linked glycosylation sites, respectively (19). To examine glycosylation status, we isolated MILL molecules from the stable transfectants by immunoprecipitation with the anti-FLAG Ab, removed

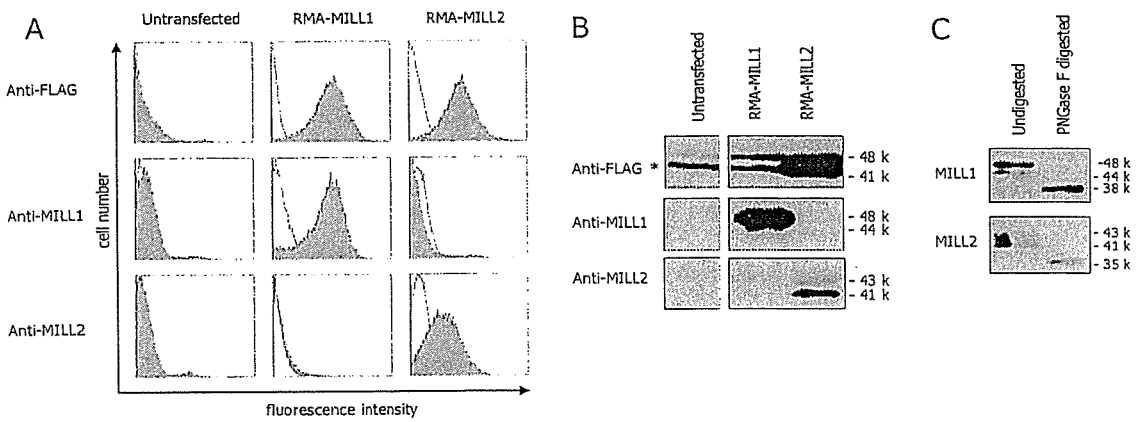

FIGURE 1. MILL1 and MILL2 are cell surface glycoproteins with *N*-linked sugars. *A*, Untransfected RMA cells and the transfected cell lines, RMA-MILL1 and RMA-MILL2, which stably express MILL1 and MILL2, respectively, were incubated with anti-FLAG mAb and FITC-conjugated goat anti-mouse IgG, anti-MILL1 antiserum (1/500 dilution) and FITC-labeled swine anti-rabbit Ig, or anti-MILL2 antiserum (1/500 dilution) and FITC-labeled swine anti-rabbit Ig (from the top to the bottom, shaded histograms). Negative control staining (open histograms) was obtained using an isotype-matched control Ab (top three panels) or normal rabbit serum (all other panels). Stained cells were analyzed by flow cytometry. *B*, Whole cell lysates of RMA-MILL1 and RMA-MILL2 were separated on 12% SDS-PAGE and subjected to immunoblotting using anti-FLAG mAb (top), anti-MILL1 antiserum (middle), or anti-MILL2 antiserum (bottom). Signals were detected by HRP-conjugated secondary Ab and ECL-Plus reagents. Nonspecific bands are indicated by asterisks. *C*, MILL1 and MILL2 proteins were immunoprecipitated with anti-FLAG mAb-coupled protein G-Sepharose beads from RMA-MILL1 and RMA-MILL2 cell lysates, respectively. After digestion with PNGase F at 37°C for 18 h, samples were separated on 12% SDS-PAGE and subjected to immunoblotting. MILL1 was detected by the rabbit anti-MILL1 antiserum and MILL2 by the rabbit anti-MILL2 antiserum. Signals were detected by HRP-conjugated secondary Ab and ECL-Plus reagents.

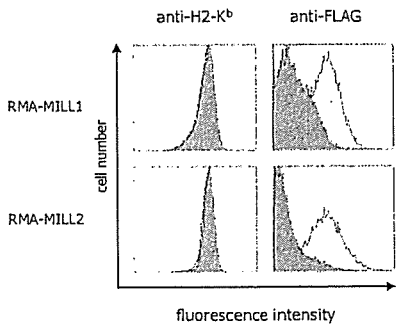

FIGURE 2. MILL1 and MILL2 are GPI-anchored proteins. RMA-MILL1 and RMA-MILL2 cells (top and bottom, respectively) were incubated with 1 U/ml PI-PLC (shaded histograms) or PBS (open histograms). Subsequently, cells were stained with anti-H2-K^b (left) or anti-FLAG (right) mAb. An FITC-conjugated F(ab')$_2$ fragment of goat anti-mouse IgG was used as a secondary Ab. Stained cells were analyzed by flow cytometry.

N-linked glycans with PNGase F and performed immunoblot analysis with the MILL-specific antisera (Fig. 1*C*). We obtained two bands of 44 and 48 kDa for non-treated MILL1, and a single band of 38 kDa for PNGase F-treated MILL1 (Fig. 1*C*, *top*). Similarly, we obtained two bands of 41 and 43 kDa for non-treated MILL2, and a single band of 35 kDa for PNGase F-treated MILL2 (Fig. 1*C*, *bottom*). The expression constructs used for stable transfection predicted M_r of 39280.83 and 35013.86 for the protein moieties of N-terminally flagged MILL1 and MILL2 molecules, respectively. Thus, the sizes of deglycosylated products agreed well with theoretical expectations. These results indicate that MILL1 and MILL2 are cell surface glycoproteins with *N*-linked sugars.

MILL1 and MILL2 are GPI-anchored proteins

We initially assumed that MILL1 and MILL2 were transmembrane proteins (19, 20). However, different prediction algorithms yielded inconsistent results concerning the presence or absence of transmembrane regions. Subsequent sequence analysis using the software 'big-PI Predictor' (25) suggested that MILL1 and MILL2 were likely GPI-anchored proteins. To examine this possibility, RMA-MILL1 and RMA-MILL2 cells were treated with PI-PLC, stained with the anti-FLAG Ab and examined by flow cytometry. In both RMA-MILL1 and RMA-MILL2 cells, cell surface staining was reduced markedly by PI-PLC treatment (Fig. 2, *right panel*). By contrast, cell surface staining with the H2-K^b Ab was not affected by similar treatment (Fig. 2, *left panel*), consistent with the fact that H2-K^b is an integral membrane protein. These results indicate that MILL1 and MILL2 are GPI-anchored cell surface proteins.

Cell surface expression of MILL molecules is TAP-independent

RMA-S is a variant derived from RMA cells (21) that lacks functional TAP molecules because of a defective TAP2 subunit (26, 27). At 37°C, classical class I molecules are barely expressed on the surface of RMA-S cells because empty class I molecules (class I molecules without peptides) are thermodynamically unstable. However, RMA-S cells express empty class I molecules when they are cultured at lower temperatures (28). To examine whether surface expression of MILL requires TAP, we transfected RMA-S cells with MILL expression plasmids and established stable transfectants. These cells were cultured at 25°C or 37°C and stained with the anti-FLAG or anti-H2-K^b Ab. As expected, endogenous H2-K^b molecules were expressed on RMA-S cells at the level comparable to that expressed on RMA cells when these cells were cultured at 25°C (Fig. 3, *A* and *B*, *left panel*, open histograms). However, expression of H2-K^b on RMA-S cells was reduced markedly when the cells were cultured at 37°C (Fig. 3, *A* and *B*, *left panel*, shaded histograms). By contrast, the expression levels of MILL1 and MILL2 detected by the anti-FLAG Ab were nearly the same regardless of whether the RMA-S cells were cultured at 25°C or 37°C (Fig. 3, *A* and *B*, *right panel*). These results indicate that cell surface expression of MILL molecules is TAP-independent.

Cell surface-expressed MILL1 and MILL2 molecules are associated with β_2m

To examine whether MILL molecules are associated with β_2m in vivo, we performed coimmunoprecipitation analysis. After treatment of RMA-MILL1 and RMA-MILL2 cells with PI-PLC, the MILL molecules released into the supernatants were immunoprecipitated with the anti-FLAG Ab and subjected to immunoblotting analysis using the anti-FLAG and anti-mouse β_2m Ab (Fig. 4). We found that β_2m was coimmunoprecipitated with both MILL1 and MILL2, indicating that MILL molecules are associated with β_2m on the cell surface.

β_2m facilitates the refolding of MILL molecules

To examine whether MILL1 and MILL2 can associate with β_2m in vitro, we expressed the extracellular domains of MILL1 and MILL2 in *E. coli* and refolded them in the presence or absence of mouse β_2m. MILL1 could be successfully refolded only in the presence of β_2m (Fig. 5*A*, *top panel*), and MILL1 and β_2m were eluted in the same fractions in gel filtration chromatography as revealed by SDS-PAGE analysis (Fig. 5*B*, *bottom half*, *top panel*). Although MILL2 was able to form soluble proteins when it was refolded in the absence of β_2m, β_2m appeared to improve the efficacy of refolding, consistent with our other results (Fig. 5*A*, *bottom panel*). MILL2 refolded in the presence of β_2m was eluted earlier in gel filtration chromatography than that refolded in the absence of β_2m (Fig. 5*A*, *bottom panel*), indicating that MILL2

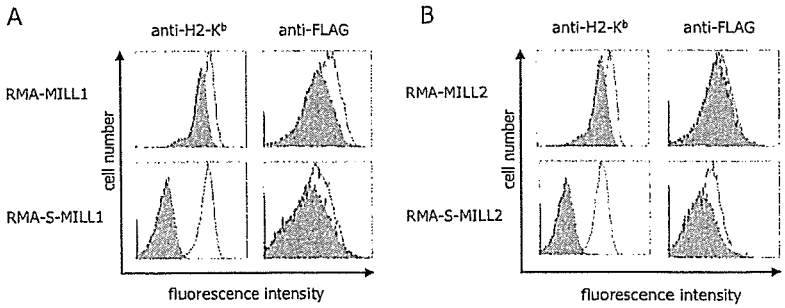

FIGURE 3. Cell surface expression of MILL molecules does not require functional TAP molecules. *A*, RMA-MILL1 and RMA-S-MILL1 cells were cultured at 25°C (open histograms) or 37°C (shaded histograms) for 18 h. Cells were incubated with anti-H2-K^b (left) or anti-FLAG (right) and then treated with FITC-conjugated F(ab')$_2$ fragments of goat anti-mouse IgG. Stained cells were analyzed by flow cytometry. *B*, RMA-MILL2 and RMA-S-MILL2 cells were treated in the same manner as in *A*, and cell surface expression of MILL2 was monitored by flow cytometry.

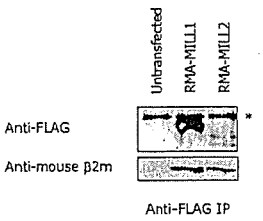

FIGURE 4. Cell surface-expressed MILL1 and MILL2 molecules are associated with β_2m. RMA-MILL1 and RMA-MILL2 cells were treated with PI-PLC and soluble MILL proteins were purified by immunoprecipitation with anti-FLAG mAb-coupled protein G-Sepharose beads (right). Precipitated samples were separated on 12% (top) or 14% (bottom) SDS-PAGE and subjected to immunoblotting analysis. MILL1 and MILL2 were detected by anti-FLAG mAb (top) whereas mouse β_2m was detected by anti-mouse β_2m Ab (bottom). Signals were detected by HRP-conjugated secondary Ab using the Super Signal West Dura kit. An asterisk indicates mouse IgG H chains.

molecules refolded in the presence of β_2m were associated with β_2m, which was further confirmed by SDS-PAGE analysis (Fig. 5*B*, *bottom panel*). MILL1 and MILL2 refolded in the presence of β_2m were purified by anion-exchange chromatography followed by gel filtration chromatography. The purified MILL1 and MILL2 proteins contained β_2m as a subunit (Fig. 5*C*). These results indicate that efficient refolding of MILL1 and MILL2 requires β_2m as a subunit. The molecular masses of MILL1/β_2m and MILL2/β_2m complexes estimated by gel filtration chromatography (Fig. 5*A*) and the relative intensities (3:1) of the MILL1 and MILL2 bands to the β_2m bands in the purified MILL1/β_2m and MILL2/β_2m complexes (Fig. 5*C*) indicate that the MILL1 or MILL2 polypeptide and β_2m bind at a 1:1 ratio.

MILL1 is expressed in a subpopulation of thymic medullary epithelial cells and a restricted region of inner root sheaths in hair follicles

To determine the tissue distribution of MILL1 and MILL2 molecules, we first performed Western blot analysis using the antisera for MILL1 and MILL2 against a panel of tissues isolated from adult and neonatal mice. These experiments yielded no bands in any tissues, presumably because the expression levels of MILL1 and MILL2 are low (data not shown). Our previous RT-PCR analysis (19) indicated that *Mill1* was transcribed in selected tissues including neonatal thymus and skin. We therefore examined expression of MILL1 in these tissues (Fig. 6). Staining was observed in a subpopulation of medullary epithelial cells in the neonatal thymus (Fig. 6*A*). These MILL1-positive cells were also detectable in the thymus of adult mice (data not shown). In the skin of 3-day-old mice, cells stained with the anti-MILL1 antiserum were found in the hair follicle (Fig. 6*B*, left). However, these cells became undetectable in the skin of 10-day-old (Fig. 6*B*, right) or 6-wk-old (not shown) mice. To more precisely address the locations of cells stained with the anti-MILL1 antiserum, we performed immunohistochemical staining of hair shafts and outer root sheaths (Fig. 6*C*). Cells stained with the anti-MILL1 antiserum were located outside the hair shaft (stained green with AE13 mAb), but inside the outer root sheath (stained green with AE1/AE3 mAb). Thus, positively stained cells are located in the inner root sheath. Because not all regions of inner root sheaths were stained with the antiserum, MILL1 seems to be expressed in a restricted region of the inner root sheath. To confirm the specificity of staining, we prepared anti-MILL1 antiserum preabsorbed with RMA-MILL1 or RMA cells. Preabsorption of the antiserum with RMA-MILL1 cells almost eliminated staining in thymic epithelial cells and hair follicles whereas staining was retained when the antiserum was preabsorbed with RMA cells (data not shown). *Mill2* is transcribed almost ubiquitously at low levels (19). We stained several tissues including neonatal thymus and skin as well as adult aorta, uterus, heart, kidney and spleen with the antiserum for MILL2 (1/200 dilution). Although this antiserum, when used at this dilution, was capable of staining RMA-MILL2 cells grown in vivo in C57BL/6 mice, we were unable to obtain any positive staining for MILL2 in any of the tissues (data not shown).

Cell surface expression of MILL1 on thymic epithelial cells requires β_2m

To examine whether cell surface expression of MILL1 requires β_2m, we isolated thymic stromal cells from 4-wk-old β_2m-deficient mice and stained with the anti-MILL1 antiserum (Fig. 7). Cell surface expression of MILL1 was almost completely abrogated in the β_2m-deficient mice compared with the adult C57BL/6 mice, indicating that cell surface expression of MILL1 is β_2m-dependent.

Discussion

MILL is the latest addition to the growing list of mammalian MHC class I families encoded outside the MHC region. Our previous work has revealed several unique features of this class I family (19, 20). First, not all mammalian species have the MILL family; although mice and rats have this family, it is absent in humans. Because MILL apparently arose before the radiation of mammals, humans seem to have lost this class I family. Second, unlike all other class I genes, the genes coding for mouse MILL have an exon between those coding for the signal peptide and the α1 domain. Third, the MILL family is phylogenetically most closely related to the MICA/B family among known class I families. Because the MILL family is absent in humans, and conversely, mice and rats lack the MICA/B family, we suggested that MILL might serve as a functional substitute of MICA/B in rodents (19). Fourth, deduced MILL molecules lack most of the residues required for the docking of peptide termini, suggesting that they are unlikely to bind peptides. Fifth, RT-PCR analysis indicated that the members of the MILL family are poorly transcribed in most adult tissues, suggesting a role other than conventional Ag presentation. Sixth, sequence comparison of rat and mouse MILL molecules revealed that *Mill* is one of the most rapidly evolving class I gene families, and that, in both *Mill1* and *Mill2*, non-synonymous substitutions occur more frequently than synonymous substitutions in the α1 domain whereas the opposite is the case in the α2 and α3 domains, suggesting that the α1 domain may be under positive selection (20). Taking all of these points into consideration, we suggested that MILL may perform specialized immune functions required only in certain species or some redundant functions, part of which are executed by other molecules (20).

In the present study, we set out to perform a biochemical characterization of mouse MILL molecules. Consistent with the absence of key residues required for the docking of peptides, we found that cell surface expression of MILL1 and MILL2 does not require functional TAP molecules (Fig. 3). Furthermore, the extracellular domains of MILL1 and MILL2 expressed in *E. coli* could be efficiently refolded in the absence of peptides under standard class I refolding conditions when β_2m was added into the mixture (Fig. 5). This is in contrast to the fact that refolding of recombinant class Ia molecules isolated from purified bacterial inclusion bodies requires the presence of a peptide ligand and is reminiscent of the behaviors of certain class Ib molecules, the refolding of which is ligand-independent (29–31). Taken together, it

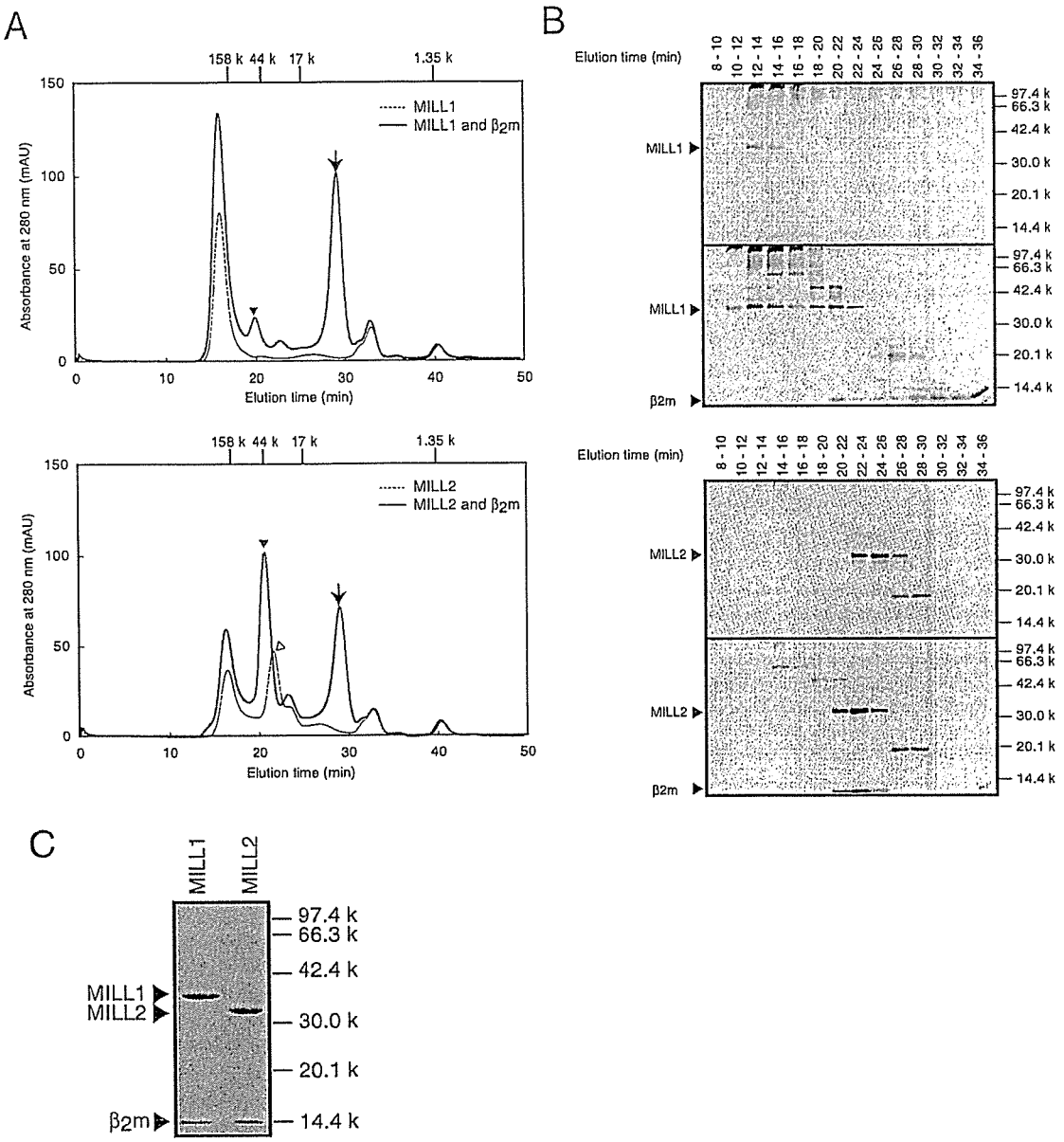

FIGURE 5. Refolding of MILL1 and MILL2 requires β_2m. *A*, Bacterially expressed extracellular domains (α1–α3) of MILL1 and MILL2 were refolded in the presence (continuous line) or absence (broken line) of β_2m and subjected to gel filtration chromatography on Superdex-75. Filled arrowheads indicate the peaks of MILL1 and MILL2 proteins associated with β_2m. Arrows indicate the peaks of free β_2m. An open arrowhead indicates the peak of MILL2 refolded in the absence of β_2m. *B*, The fractions from gel filtration chromatography were analyzed on SDS-PAGE, and the gels were stained with silver staining. The top and bottom halves of each panel indicate fractionation of the samples refolded in the absence and presence of β_2m, respectively. *C*, Coomassie brilliant blue-stained SDS-PAGE gel of in vitro refolded MILL1 and MILL2 molecules purified by sequential chromatography.

is likely that the MILL family of class I molecules performs functions other than the presentation of peptides.

Two observations made in this work were rather unexpected. First, we initially assumed that, like most other class I family members, MILL1 and MILL2 were integral membrane proteins with a transmembrane region (19, 20). Contrary to this assumption, MILL1 and MILL2 turned out to be GPI-anchored proteins (Fig. 2). The occurrence of GPI anchors is not unprecedented for class I molecules because most if not all members of RAE-1 and ULBP families as well as a large proportion of Qa-2 molecules are GPI-anchored (32–35). Like other GPI-anchored proteins (36, 37), MILL may be primarily located in lipid rafts. Second, we assumed that MILL1 and MILL2 were unlikely to be associated with β_2m because they lack many of the residues known to interact with β_2m in classical class I molecules (19). Our present work demonstrates that both MILL1 and MILL2 are associated with β_2m on the cell surface (Fig. 4). A similar unexpected association with β_2m was previously observed for MR1; this class Ib molecule lacks many of the phylogenetically conserved motifs implicated in β_2m association in class Ia molecules (38), yet biochemical studies have revealed that it associates with β_2m (38, 39). We also found that β_2m promoted refolding of bacterially produced MILL ectodomains in vitro (Fig. 5). Hence, β_2m appears to constitute an integral component of MILL class I molecules. Consistent with this, cell surface expression of MILL1 on thymic stromal cells was almost completely abrogated in β_2m-deficient mice, indicating that cell

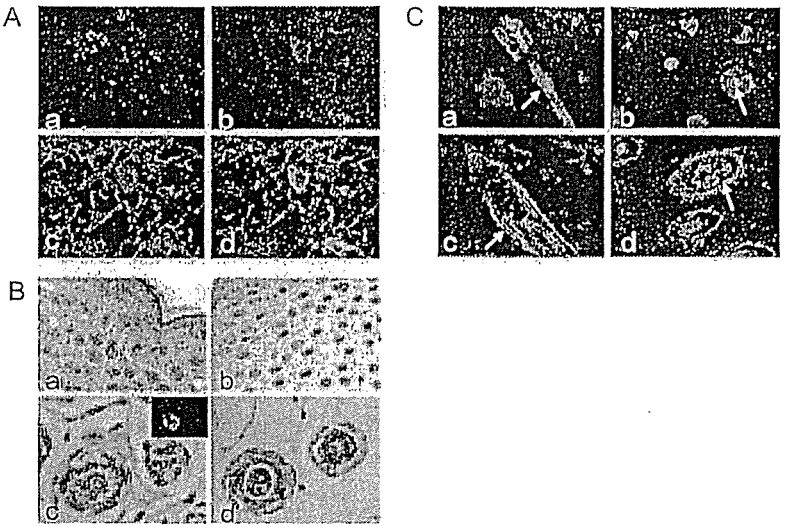

FIGURE 6. MILL1 is likely expressed in thymic medullary epithelial cells and hair follicles. *A*, Thymic tissue sections obtained from 3-day-old mice were blocked by incubation with normal goat serum (1/500 dilution), reacted with AE1/AE3 and anti-MILL1 (1/400 dilution) followed by staining with Alexa Fluor 488-conjugated goat anti-mouse IgG (1/300 dilution) and Alexa Fluor 594-conjugated goat anti-rabbit IgG (1/300 dilution). *Aa*, a low-power photo micrograph of the thymic medulla (original magnification ×100); *Ab–Ad*, a high-power magnification (original magnification ×400). Images for MILL1 (stained red, *Ab*) and AE1/AE3 (stained green, *Ac*) as well as the merged image (*Ad*) were obtained with a Nikon ECLIPSE E600 microscope. *B*, Skin tissues of 3-day-old (*Ba* and *Bc*) and 10-day-old (*Bb* and *Bd*) mice. *Upper panels*, H&E (original magnification ×100). *Lower panels*, H&E (original magnification ×400). The inset in *Bc* shows staining with the anti-MILL1 antiserum (original magnification ×100). Staining was done as described in the legend to *C*. *C*, MILL1 is likely expressed in cells of the inner root sheaths. In *Ca* and *Cb*, tissue sections were blocked by incubation with normal goat serum (1/500 dilution), reacted with AE13 (1/1000 dilution) and anti-MILL1 (1/400 dilution) and stained with Alexa Fluor 488-conjugated goat anti-mouse IgG (1/300 dilution) and Alexa Fluor 594-conjugated goat anti-rabbit IgG (1:300 dilution). In *Cc* and *Cd*, AE13 was substituted by AE1/AE3. MILL1 is stained red. The hair cortex (*Ca* and *Cb*) and outer root sheaths (*Cc* and *Cd*) are stained green. In *Ca* and *Cc*, hair shafts were sectioned parallel to the long axis. *Cb* and *Cd* show cross sections of hair shafts. Arrows in *Ca* and *Cb* indicate the hair cortex, whereas those in *Cc* and *Cd* indicate outer root sheaths. Original magnification ×400.

surface expression of MILL1 requires β_2m (Fig. 7). Given the overall structural similarity of MILL1 and MILL2 (19), and their shared biochemical properties (Figs. 2–5), it seems reasonable to assume that MILL2 also requires β_2m for cell surface expression. Because the refolding experiments showed that MILL2, but not MILL1, was able to form soluble proteins in the absence of β_2m, albeit much less efficiently than in the presence of β_2m (Fig. 5), β_2m might not be an absolute requirement for cell surface expression of MILL2. Human CD1d molecules, normally associated with β_2m, can be expressed on the surface of intestinal epithelial cells in a β_2m-independent manner (40, 41), indicating that the requirement for β_2m can differ depending on tissues. Therefore, it will be necessary to identify cells or tissues where MILL2 is physiologically expressed to determine whether cell surface expression of MILL2 requires β_2m in vivo, and if it does, whether β_2m is absolutely required.

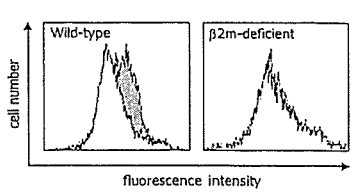

FIGURE 7. Cell surface expression of MILL1 requires β_2m. Thymic stromal cells isolated from C57BL/6 (*left panel*) and β_2m-deficient (*right panel*) mice were stained with normal rabbit serum (open histograms) or the rabbit anti-MILL1 antiserum (shaded histograms). An FITC-labeled swine anti-rabbit Ig was used as a secondary Ab. Stained cells were analyzed by flow cytometry.

Immunohistochemical analysis showed that MILL1 is expressed in a subpopulation of thymic medullary epithelial cells and a restricted region of inner root sheaths in hair follicles (Fig. 6). Expression in the thymus is suggestive of an immunological role for MILL1. Totally unexpected was the observation that some inner root sheath cells in 3-day-old, but not 10-day-old or 6-wk-old, mice were stained with the antiserum for MILL1, although we cannot rule out the possibility that our anti-MILL1 antiserum cross-reacts with epitopes on unrelated molecules in hair follicles. Hair follicles have been proposed to enjoy immune privilege (42, 43). Thus, MILL1 may somehow be involved in the establishment and maintenance of immune privilege in hair follicles. On the other hand, we have thus far been unable to identify cells expressing MILL2 proteins despite the fact that the *Mill2* gene is ubiquitously transcribed at low levels. Thus, expression of MILL2 proteins might be translationally regulated or MILL2 proteins might be expressed at detectable levels only in highly specialized cells as recently demonstrated for certain class I molecules (16, 17). It is also possible that expression of the MILL family is enhanced by certain stimuli or under pathologic conditions. To fully understand the expression patterns of the MILL family, more detailed analysis is required.

In conclusion, this study highlights the biochemical differences between the MILL and MICA/B families of class I molecules. MILL1 and MILL2 are TAP-independent, β_2m-associated glycoproteins attached to the cell surface by GPI anchors. In contrast, MICA and MICB are TAP-independent, transmembrane proteins that do not associate with β_2m (44). These two families of class I molecules also differ in their expression patterns. MICA and MICB are stress-inducible class I molecules usually not expressed

on the surface of normal cells (44). In contrast, expression of *Mill1* or *Mill2* mRNA is not inducible by heat shock (our unpublished observation), and the expression in hair follicles seems unique to the MILL family. Furthermore, our preliminary work indicates that NK cells are not stained with MILL tetramers. All of these observations argue against the possibility that MILL is a functional substitute of MICA/B in rodents. Generation of knockout mice may provide a clue for understanding the biologic function of the MILL family.

Acknowledgments

We gratefully acknowledge Dr. Taeko Nagata and Kaori Kuno for technical assistance.

Disclosures

The authors have no financial conflict of interest.

References

1. Bjorkman, P. J., and P. Parham. 1990. Structure, function, and diversity of class I major histocompatibility complex molecules. *Annu. Rev. Biochem.* 59: 253–288.
2. Klein, J. 1986. *Natural History of the Major Histocompatibility Complex*. John Wiley & Sons, New York.
3. Klein, J., and C. O'hUigin. 1994. The conundrum of nonclassical major histocompatibility complex genes. *Proc. Natl. Acad. Sci. USA* 91: 6251–6252.
4. Rodgers, J. R., and R. G. Cook. 2005. MHC class Ib molecules bridge innate and acquired immunity. *Nat. Rev. Immunol.* 5: 459–471.
5. Radosavljevic, M., and S. Bahram. 2003. In vivo immunogenetics: from *MIC* to *RAET1* loci. *Immunogenetics* 55: 1–9.
6. Bahram, S., M. Bresnahan, D. E. Geraghty, and T. Spies. 1994. A second lineage of mammalian major histocompatibility complex class I genes. *Proc. Natl. Acad. Sci. USA* 91: 6259–6263.
7. Araki, T., F. Gejyo, K. Takagaki, H. Haupt, H. G. Schwick, W. Buergi, T. Marti, J. Schaller, E. Rickli, R. Brossmer, et al. 1988. Complete amino acid sequence of human plasma Zn-α2-glycoprotein and its homology to histocompatibility antigens. *Proc. Natl. Acad. Sci. USA* 85: 679–683.
8. Fukudome, K., and C. T. Esmon. 1994. Identification, cloning, and regulation of a novel endothelial cell protein C/activated protein C receptor. *J. Biol. Chem.* 269: 26486–26491.
9. Zou, Z., M. Nomura, Y. Takihara, T. Yasunaga, and K. Shimada. 1996. Isolation and characterization of retinoic acid-inducible cDNA clones in F9 cells: a novel cDNA family encodes cell surface proteins sharing partial homology with MHC class I molecules. *J. Biochem.* 119: 319–328.
10. Fischer Lindahl, K., E. Hermel, B. E. Loveland, and C. R. Wang. 1991. Maternally transmitted antigen of mice: a model transplantation antigen. *Annu. Rev. Immunol.* 9: 351–372.
11. Treiner, E., L. Duban, S. Bahram, M. Radosavljevic, V. Wanner, F. Tilloy, P. Affaticati, S. Gilfillan, and O. Lantz. 2003. Selection of evolutionarily conserved mucosal-associated invariant T cells by MR1. *Nature* 422: 164–169.
12. Vincent, M. S., J. E. Gumperz, and M. B. Brenner. 2003. Understanding the function of CD1-restricted T cells. *Nat. Immunol.* 4: 517–523.
13. Bahram, S. 2000. MIC genes: from genetics to biology. *Adv. Immunol.* 76: 1–60.
14. Cerwenka, A., and L. L. Lanier. 2001. Natural killer cells, viruses and cancer. *Nat. Rev. Immunol.* 1: 41–49.
15. Simister, N. E., and K. E. Mostov. 1989. An Fc receptor structurally related to MHC class I antigens. *Nature* 337: 184–187.
16. Ishii, T., J. Hirota, and P. Mombaerts. 2003. Combinatorial coexpression of neural and immune multigene families in mouse vomeronasal sensory neurons. *Curr. Biol.* 13: 394–400.
17. Loconto, J., F. Papes, E. Chang, L. Stowers, E. P. Jones, T. Takada, A. Kumanovics, K. Fischer Lindahl, and C. Dulac. 2003. Functional expression of murine V2R pheromone receptors involves selective association with the M10 and M1 families of MHC class Ib molecules. *Cell* 112: 607–618.
18. Todorov, P. T., T. M. McDevitt, D. J. Meyer, H. Ueyama, I. Ohkubo, and M. J. Tisdale. 1998. Purification and characterization of a tumor lipid-mobilizing factor. *Cancer Res.* 58: 2353–2358.
19. Kasahara, M., Y. Watanabe, M. Sumasu, and T. Nagata. 2002. A family of MHC class I-like genes located in the vicinity of the mouse leukocyte receptor complex. *Proc. Natl. Acad. Sci. USA* 99: 13687–13692.
20. Watanabe, Y., T. Maruoka, L. Walter, and M. Kasahara. 2004. Comparative genomics of the *Mill* family: a rapidly evolving MHC class I gene family. *Eur. J. Immunol.* 34: 1597–1607.
21. Karre, K., H. G. Ljunggren, G. Piontek, and R. Kiessling. 1986. Selective rejection of H-2-deficient lymphoma variants suggests alternative immune defence strategy. *Nature* 319: 675–678.
22. Wada, H., N. Matsumoto, K. Maenaka, K. Suzuki, and K. Yamamoto. 2004. The inhibitory NK cell receptor CD94/NKG2A and the activating receptor CD94/NKG2C bind the top of HLA-E through mostly shared but partly distinct sets of HLA-E residues. *Eur. J. Immunol.* 34: 81–90.
23. Baba, T., A. Ishizu, H. Ikeda, Y. Miyatake, T. Tsuji, A. Suzuki, U. Tomaru, and T. Yoshiki. 2005. Chronic graft-versus-host disease-like autoimmune disorders spontaneously occurred in rats with neonatal thymus atrophy. *Eur. J. Immunol.* 35: 1731–1740.
24. Gray, D. H., A. P. Chidgey, and R. L. Boyd. 2002. Analysis of thymic stromal cell populations using flow cytometry. *J. Immunol. Methods* 260: 15–28.
25. Eisenhaber, B., P. Bork, and F. Eisenhaber. 1999. Prediction of potential GPI-modification sites in proprotein sequences. *J. Mol. Biol.* 292: 741–758.
26. Attaya, M., S. Jameson, C. K. Martinez, E. Hermel, C. Aldrich, J. Forman, K. F. Lindahl, M. J. Bevan, and J. J. Monaco. 1992. Ham-2 corrects the class I antigen-processing defect in RMA-S cells. *Nature* 355: 647–649.
27. Yang, Y., K. Fruh, J. Chambers, J. B. Waters, L. Wu, T. Spies, and P. A. Peterson. 1992. Major histocompatibility complex (MHC)-encoded HAM2 is necessary for antigenic peptide loading onto class I MHC molecules. *J. Biol. Chem.* 267: 11669–11672.
28. Ljunggren, H. G., N. J. Stam, C. Ohlen, J. J. Neefjes, P. Hoglund, M. T. Heemels, J. Bastin, T. N. Schumacher, A. Townsend, K. Karre, et al. 1990. Empty MHC class I molecules come out in the cold. *Nature* 346: 476–480.
29. Li, P., G. McDermott, and R. K. Strong. 2002. Crystal structures of RAE-1β and its complex with the activating immunoreceptor NKG2D. *Immunity* 16: 77–86.
30. Steinle, A., P. Li, D. L. Morris, V. Groh, L. L. Lanier, R. K. Strong, and T. Spies. 2001. Interactions of human NKG2D with its ligands MICA, MICB, and homologs of the mouse RAE-1 protein family. *Immunogenetics* 53: 279–287.
31. Wingren, C., M. P. Crowley, M. Degano, Y. Chien, and I. A. Wilson. 2000. Crystal structure of a γδ T cell receptor ligand T22: a truncated MHC-like fold. *Science* 287: 310–314.
32. Nomura, M., Z. Zou, T. Joh, Y. Takihara, Y. Matsuda, and K. Shimada. 1996. Genomic structures and characterization of Rae1 family members encoding GPI-anchored cell surface proteins and expressed predominantly in embryonic mouse brain. *J. Biochem.* 120: 987–995.
33. Stiernberg, J., M. G. Low, L. Flaherty, and P. W. Kincade. 1987. Removal of lymphocyte surface molecules with phosphatidylinositol-specific phospholipase C: effects on mitogen responses and evidence that ThB and certain Qa antigens are membrane-anchored via phosphatidylinositol. *J. Immunol.* 138: 3877–3884.
34. Cerwenka, A., A. B. Bakker, T. McClanahan, J. Wagner, J. Wu, J. H. Phillips, and L. L. Lanier. 2000. Retinoic acid early inducible genes define a ligand family for the activating NKG2D receptor in mice. *Immunity* 12: 721–727.
35. Cosman, D., J. Mullberg, W. Chin, R. Armitage, W. Fanslow, M. Kubin, and N. J. Chalupny. 2001. ULBPs, novel MHC class I-related molecules, bind to CMV glycoprotein UL16 and stimulate NK cytotoxicity through the NKG2D receptor. *Immunity* 14: 123–133.
36. Horejsi, V., K. Drbal, M. Cebecauer, J. Cerny, T. Brdicka, P. Angelisova, and H. Stockinger. 1999. GPI-microdomains: a role in signalling via immunoreceptors. *Immunol. Today* 20: 356–361.
37. Pizzo, P., and A. Viola. 2004. Lipid rafts in lymphocyte activation. *Microbes Infect.* 6: 686–692.
38. Miley, M. J., S. M. Truscott, Y. Y. Yu, S. Gilfillan, D. H. Fremont, T. H. Hansen, and L. Lybarger. 2003. Biochemical features of the MHC-related protein 1 consistent with an immunological function. *J. Immunol.* 170: 6090–6098.
39. Yamaguchi, H., and K. Hashimoto. 2002. Association of MR1 protein, an MHC class I-related molecule, with β_2-microglobulin. *Biochem. Biophys. Res. Commun.* 290: 722–729.
40. Balk, S. P., S. Burke, J. E. Polischuk, M. E. Frantz, L. Yang, S. Porcelli, S. P. Colgan, and R. S. Blumberg. 1994. β_2-microglobulin-independent MHC class Ib molecule expressed by human intestinal epithelium. *Science* 265: 259–262.
41. Somnay-Wadgaonkar, K., A. Nusrat, H. S. Kim, W. P. Canchis, S. P. Balk, S. P. Colgan, and R. S. Blumberg. 1999. Immunolocalization of CD1d in human intestinal epithelial cells and identification of a β_2-microglobulin-associated form. *Int. Immunol.* 11: 383–392.
42. Niederkorn, J. Y. 2003. Mechanisms of immune privilege in the eye and hair follicle. *J. Investig. Dermatol. Symp. Proc.* 8: 168–172.
43. Paus, R., B. J. Nickoloff, and T. Ito. 2005. A 'hairy' privilege. *Trends Immunol.* 26: 32–40.
44. Groh, V., S. Bahram, S. Bauer, A. Herman, M. Beauchamp, and T. Spies. 1996. Cell stress-regulated human major histocompatibility complex class I gene expressed in gastrointestinal epithelium. *Proc. Natl. Acad. Sci. USA* 93: 12445–12450.

$CD4^+/CD8^+$ macrophages infiltrating at inflammatory sites: a population of monocytes/macrophages with a cytotoxic phenotype

Tomohisa Baba, Akihiro Ishizu, Sari Iwasaki, Akira Suzuki, Utano Tomaru, Hitoshi Ikeda, Takashi Yoshiki, and Masanori Kasahara

We found a population of nonlymphoid cells expressing both CD4 and CD8 in peripheral blood mononuclear cells (PBMCs) of human T-cell leukemia virus type-I *pX* transgenic rats with autoimmune diseases. These cells, which showed a monocytic phenotype, were also found in wild-type rats, and their number increased by adjuvant-assisted immunization. GM-CSF increased the number of these double-positive (DP) monocytes in PBMCs. Consistent with the idea that DP monocytes differentiate into DP macrophages at sites of inflammation, we found infiltration of DP macrophages at the site of myosin-induced myocarditis in wild-type rats; these cells exhibited a T-helper 1 (Th1)–type cytokine/chemokine profile and expressed high levels of Fas ligand, perforin, granzyme B, and NKR-P2 (rat orthologue of human NKG2D). Adoptive transfer of GFP-positive spleen cells confirmed hematogenous origin of DP macrophages. DP monocytes had a cytotoxic phenotype similar to DP macrophages, indicating that this phenotypic specialization occurred before entry into a tissue. In line with this, DP monocytes killed tumor cells in vitro. Combined evidence indicates that certain inflammatory stimuli that induce GM-CSF trigger the expansion of a population of DP monocytes with a cytotoxic phenotype and that these cells differentiate into macrophages at inflammatory sites. Interestingly, human PBMCs also contain DP monocytes. (Blood. 2006;107:2004-2012)

Introduction

Despite their origin from a common bone marrow progenitor population, cells of the monocyte/macrophage lineage display considerable phenotypic and functional heterogeneity. Thus, macrophages residing in the liver and the lungs differ in their basal activity as well as their ability to respond to inflammatory mediators. Even within a single organ, macrophages are heterogeneous; macrophages localized in the centrilobular and periportal regions of the liver differ in size, the ability to produce superoxide anion, and phagocytic activities.[1] In an inflammatory response, the early stages are dominated by macrophages showing inflammatory and tissue-destructive activities, and, in the late stages, macrophages with tissue-restructuring activities predominate.[2] In tumor tissues, infiltrating macrophages tend to acquire a polarized M2 phenotype, promoting tumor growth and progression.[3] Accumulated evidence indicates that such macrophage heterogeneity is largely attributable to microenvironmental signals including cytokines and microbial products. Although this suggests that macrophages do not have stable, lineage-defined subsets and that their functional phenotypes change in response to a microenvironment, definitions of macrophage subpopulations are important not only for understanding their role in host defense and disease pathogenesis but also for designing effective therapeutic interventions.

In our previous study, we made F1 rats by mating F344 transgenic rats expressing the human T-cell leukemia virus type-I (HTLV-I) *pX* gene[4] to nontransgenic Wistar rats and found that they developed disorders, including atrophy of the thymus, lymphocytopenia, and inflammatory cell infiltration into multiple organs, as typically seen in chronic graft-versus-host disease (GVHD).[5] In these rats (hereafter referred to as FW-pX rats), the HTLV-I *pX* transgene induced neonatal apoptosis of the thymic epithelial cells, resulting in lymphocytopenia accompanied by compensatory expansion of peripheral myeloid cells, production of autoreactive T cells, and subsequent development of chronic GVHD-like autoimmune diseases.

In the present study, we found that a population of monocytic cells expressing both CD4 and CD8 was expanded in the peripheral blood of FW-pX rats. Monocytes/macrophages constitutively express CD4 in humans and rats[6,7] but not in mice. On the other hand, some myeloid cells including natural killer (NK) cells, mast cells, macrophages, and dendritic cells (DCs) express CD8.[8-14] We therefore hypothesized that rat peripheral blood contains a population of monocytes expressing both CD4 and CD8 and that this population is expanded under certain activating conditions. To test this hypothesis, we used a rat model of myosin-induced myocarditis. Here we show that the number of CD4/CD8 double-positive (DP) monocytes is indeed increased by adjuvant-assisted immunization with myosin or by administration of adjuvants alone and that these cells express cytotoxic factors such as perforin and granzyme B and exhibit cytotoxicity against tumor cells in vitro. Approximately half of the macrophages that infiltrated the cardiac lesion expressed both CD4 and CD8; these DP macrophages, shown to be of hematogenous origin by adoptive transfer experiments, expressed Fas ligand (Fas L), perforin, and granzyme B at high levels. Thus, our present work demonstrates the existence of a distinct population of monocytes/macrophages characterized

From the Department of Pathology/Pathophysiology, Division of Pathophysiological Science, Hokkaido University Graduate School of Medicine, Sapporo, Japan.

Submitted June 16, 2005; accepted October 17, 2005. Prepublished online as *Blood* First Edition Paper, November 3, 2005; DOI 10.1182/blood-2005-06-2345.

Supported by grants from the Ministries of Education, Culture, Sports, Science, and Technology and of Health, Labor, and Welfare, of Japan.

Reprints: Akihiro Ishizu, Department of Pathology/Pathophysiology, Division of Pathophysiological Science, Hokkaido University Graduate School of Medicine, Kita-15, Nishi-7, Kita-ku, Sapporo 060-8638, Japan; e-mail: aishizu@med.hokudai.ac.jp.

The publication costs of this article were defrayed in part by page charge payment. Therefore, and solely to indicate this fact, this article is hereby marked "advertisement" in accordance with 18 U.S.C. section 1734.

by coexpression of CD4 and CD8 and by a cytotoxic phenotype. Interestingly, human peripheral blood also contains DP monocytes.

Materials and methods

Rats

FW-pX rats were obtained by mating male F344 transgenic rats expressing the HTLV-I *pX* gene without any tissue specificity (line 38)[4] to nontransgenic female Wistar rats. Offspring were screened for the *pX* transgene by genomic polymerase chain reaction (PCR) as described.[4] FW–wild-type (FW-wt) rats were obtained by mating nontransgenic male F344 rats to female Wistar rats. HTLV-I *pX* transgenic rats (line 38) were maintained at the Institute of Animal Experimentation, Hokkaido University Graduate School of Medicine. Inbred F344 and closed-colony Wistar rats were purchased from SLC (Shizuoka, Japan) and Charles River (Kanagawa, Japan), respectively. The EGFP transgenic rats that ubiquitously expressed green fluorescent protein (GFP)[15] were obtained from the YS Institute (Utsunomiya, Japan) and Tohoku University (Sendai, Japan). All experiments using rats were done according to the Guideline for the Care and Use of Laboratory Animals in Hokkaido University Graduate School of Medicine.

Human blood samples

Human blood samples were obtained from 12 healthy donors after informed consent and used for flow cytometry (FCM). None of the donors had medical histories of autoimmune diseases, recent infection, or neoplasms.

Antibodies

Murine monoclonal antibodies (Abs) used were anti–rat CD3 (IF4 for immunohistochemistry, Cedarlane, Hornby, ON, Canada; and G4.18 for FCM, Pharmingen, San Diego, CA), anti–rat CD4 (OX-35; Pharmingen), anti–rat CD8 α-chain hinge region (OX-8; Pharmingen), anti–rat CD8 α-chain immunoglobulin (Ig) V–like region (G28; Pharmingen), anti–rat CD8 β-chain (341; Pharmingen), anti–rat CD11b/c (OX-42; Pharmingen), anti–rat CD68 (ED-1; Serotec, Oxford, United Kingdom), anti–rat CD163 (ED-2; Serotec), anti–rat B cell (RLN-9D3; Serotec), anti–rat DC (OX-62; Cedarlane), and NKR-P1A (10/78; Pharmingen), as well as anti–human CD4 (M-T466; Miltenyi Biotec, Bergisch Gladbach, Germany), anti–human CD8 (HIT8a; Pharmingen), and anti–human CD14 (MφP9; Pharmingen). Polyclonal rabbit anti–Fas L (N-20) and goat anti–granzyme B (N-19) Abs were purchased from Santa Cruz Biotechnology (Santa Cruz, CA). Mouse IgG1 or IgG2 (CBL600P or CBL601P, respectively; Chemicon International, Temecula, CA) and rabbit or goat IgG (Sigma-Aldrich, St Louis, MO) served as controls.

Recombinant cytokines/chemokines

Recombinant cytokines/chemokines used were rat RANTES and GM-CSF (PEPROTECH EC, London, United Kingdom) and mouse IL-12 (R&D Systems, Minneapolis, MN) previously shown to function in rats.[16] For in vivo administration, GM-CSF (1.0 μg per 1 mL PBS) was injected intravenously into 6-week-old Wistar rats. Peripheral blood was assayed 24 hours after injection.

FCM and MACS

Peripheral blood cells were stained by the direct method without removal of serum. After reaction with Abs, erythrocytes were depleted by treatment with ammonium chloride. Expression of cell surface molecules was analyzed using FACScan (Becton Dickinson, Franklin Lakes, NJ) with CellQuest software (Becton Dickinson). Magnetic-activated cell sorting (MACS) was done using Magnetic Cell Separator (Miltenyi Biotec) as described.[17]

Phagocytosis assay

Yellow-green carboxylate-modified 1.0 μm latex beads (Sigma-Aldrich) were mixed with rat peripheral blood (1.5×10^7 beads/300 μL blood). After incubation for 2 hours at 37°C, PE-conjugated anti-CD4 (OX-35) and PerCP-conjugated anti-CD8 (OX-8) Abs were added to the mixture, followed by depletion of erythrocytes using ammonium chloride. After 3 times wash with cold PBS, $CD4^+/CD8^+$ DP cells were gated to determine uptake of the fluorescence-labeled beads using FACScan.

Immunization of rats with porcine heart myosin and induction of myocarditis

Killed tuberculosis germs were added to Freund incomplete adjuvant (Sigma-Aldrich) to reach the concentration of 100 mg/mL. Two milligrams of myosin from porcine heart (Sigma-Aldrich) were emulsified with an equal volume (200 μL) of the prepared adjuvant. The emulsion containing porcine myosin was inoculated into bilateral footpads of 3-week-old FW-wt rats (200 μL/site).

Histopathology and immunohistochemistry

Tissue samples were fixed in 10% phosphate-buffered formaldehyde and embedded in paraffin blocks. Each 4-μm section was stained with hematoxylin and eosin. For immunohistochemistry, an avidin-biotin immunoperoxidase kit (DAKO, Glostrup, Denmark) was used. After immunostaining, tissue sections were counterstained with Mayer hematoxylin (Merck, Darmstadt, Germany).

Isolation of macrophages from cardiac tissues with myocarditis

At 3 weeks after myosin immunization, the heart was extirpated and then perfused by PBS ex vivo. The cardiac tissues were cut into small pieces and digested by 0.16% collagenase type II (Worthington Biochemical Corporation, Lakewood, NJ). After removal of tissue fragments, cell suspension was incubated in a plastic dish at 37°C. One hour later, adherent cells were harvested and used as tissue-infiltrating macrophages. The purity of ED-1–positive ($CD68^+$) positive cells regarded as macrophages was 94% (data not shown).

Immunocytochemistry

Mononuclear cells separated from rat spleen using Histopaque-1083 (Sigma-Aldrich) or isolated from cardiac tissues were cultured in chamber slides (Nalge Nunc International, Roskilde, Denmark) for 1 hour. Resultant adherent cells were fixed using cold acetone for 5 minutes or 4% paraformaldehyde for 15 minutes at room temperature and then stained by the standard method (for details, see the legends of Figures 2 and 4-6). After washing with PBS, the slides were mounted in fluorescent mounting medium (DAKO). Immunofluorescence was detected using a confocal microscope (MRC-1024; BIO-RAD, Hercules, CA) or a fluorescence microscope (ECLIPSE E600; Nikon, Tokyo, Japan).

Image processing

Microscopic photographs were taken using the objective lens (40 ×/0.75 numeric aperture) in the DP70 system (Olympus, Tokyo, Japan). DP Controller software (Olympus) was used for image processing.

RT-PCR and quantitative real-time RT-PCR

Total RNAs were extracted from cells by RNeasy Mini Kit (QIAGEN, Alameda, CA) and then reverse transcribed using M-MLV reverse transcriptase (Invitrogen, Paisley, United Kingdom). PCR was performed using the cDNAs, 2 mM dNTP mix (GeneAmp dNTPMix; Applied Biosystems, Foster City, CA), *Taq* DNA polymerase kit (AmpliTaq Gold; Applied Biosystems), and primer sets for 28 cycles of 95°C 1 minute, 56°C 1 minute, and 72°C 1 minute. Quantitative real-time reverse transcription–PCR (RT-PCR) was performed using the cDNAs, QuantiTec SYBR Green PCR Kit (QIAGEN), and primer sets. Relative expression of target genes was analyzed using the ΔΔCT method.[18] The expression level of the *Gapdh* (glyceraldehyde-3-phosphate dehydrogenase) gene was used as an internal control. PCR was conducted for 40 cycles using an ABI PRISM 7000 Sequence Detector System (Applied Biosystems) with 2-step reactions

Table 1. Primer sets used for RT-PCR and quantitative real-time RT-PCR

Gene	Forward	Reverse
Cd3	5′-CGAATGTGCCAGAACTGTGT-3′	5′-AGTGTCAACAGCCCCAGAAA-3′
Fas ligand (*Fasl*)	5′-GCCCGTGAATTACCCATGTC-3′	5′-TGGAGGAGCCCAAGGAGAA-3′
Gapdh	5′-ATGGGAGTTGCTGTTGAAGTCA-3′	5′-CCGAGGGCCCACTAAAGG-3′
Granzyme B (*Gzmb*)	5′-GGCCCACAACATCAAAGAAC-3′	5′-CGCTAGACCTCTTGGCCTTAC-3′
Ifng	5′-GATCCAGCACAAAGCTGTCA-3′	5′-GACTCCTTTTCCGCTTCCTT-3′
Il4	5′-TGTACCTCCGTGCTTGAAGA-3′	5′-GTGAGTTCAGACCGCTGACA-3′
Il12	5′-AGGTGCGTTCCTCGTAGAGA-3′	5′-CCATTTGCTGCATGATGAAT-3′
Il18	5′-ACCGCAGTAATACGGAGCAT-3′	5′-GTTGGCTGTTCGGTCGATA-3′
Nos2	5′-TCTGCAGCACTTGGATCAAT-3′	5′-AGCTGGAAGCCACTGACACT-3′
MCP-1 (*Ccl2*)	5′-TGTCTCAGCCAGATGCAGTT-3′	5′-TGCTGCTGGTGATTCTCTTG-3′
MDC (*Ccl22*)	5′-TGGCTCTCGTCCTTCTTGTT-3′	5′-TCTTCCACATTGGCACCATA-3′
Nkrp2	5′-TGACATGGCTTGCTGTTTTC-3′	5′-TGGTTCCAGGCTTTGTTCTC-3′
Perforin 1 (*Prf1*)	5′-TTGCGAGGAGAAGAAGAAACA-3′	5′-CGGTAGGTCTGGTGGAAAGA-3′
RANTES (*Ccl5*)	5′-GTGCCCACGTGAAGGAGTAT-3′	5′-ACTGCAAGGTTGGAGCACTT-3′
Tgfb1	5′-ATACGCCTGAGTGGCTGTCT-3′	5′-TGAAGCGAAAGCCCTGTATT-3′
Tnfa	5′-GTGCCTCAGCCTCTTCTCAT-3′	5′-CAATCACCCCGAAGTTCAGT-3′

(95°C for 30 s, 60°C for 30 s) after initial denaturation of 95°C for 15 minutes. The primer sequences for PCR are listed in Table 1.

Transfer of GFP-positive spleen cells into nontransgenic recipients

The EGFP transgenic rats and nontransgenic Wistar rats (all rats were 4 weeks old) were immunized with porcine myosin as described under "Immunization of rats with porcine heart myosin and induction of myocarditis." Mononuclear cells were isolated from the spleen of EGFP transgenic rats one week after immunization and transferred into Wistar rats that had been immunized with myosin 2 weeks before (1×10^7/rat intravenously). Five days later, the hearts of the recipients were extirpated, and tissue-infiltrating macrophages were isolated.

Cytotoxic assay

Six-week-old Wistar rats were immunized with adjuvants containing killed tuberculosis germs. One week later, mononuclear cells were separated from the spleen and incubated in plastic dishes for 20 minutes at 37°C. Resultant adherent cells were collected and then divided into $CD8^-$ and $CD8^+$ cells using the MACS system. These cells were added to the culture of allogenic epithelial thymoma cells (originated from F344 rats carrying the HTLV-I *pX* transgene[19]) with effector-target (E/T) ratios of 30, 10, 1, and 0.1 (4×10^4 target cells per well in 24-well plates). After incubation for 18 hours, cytotoxicity was measured using the CytoTox 96 test kit (Promega, Madison, WI).

Statistical analysis

Data were represented as mean ± standard deviation (SD). Statistical significance between any 2 groups was determined by 2-tailed Student *t* test. *P* values less than .05 were considered to be significant.

Results

Expansion of $CD4^+/CD8^+$ cells in the peripheral blood of FW-pX rats with chronic GVHD-like autoimmune diseases

In FW-pX rats, the HTLV-I *pX* transgene induced atrophy of the thymus, resulting in lymphocytopenia, production of autoreactive T cells, and subsequent development of chronic GVHD-like autoimmune diseases.[5] These rats also displayed a compensatory increase in the number of peripheral myeloid cells. To characterize immunophenotypic alterations in their peripheral blood mononuclear cells (PBMCs), we performed 2-color FCM analysis using PBMCs isolated from 6-week-old FW-pX and age-matched control FW-wt rats (Figure 1). The percentages of $CD4^+/CD8^-$ and $CD4^-/CD8^+$ T cells (6.1% and 9.9%, respectively) in FW-pX rats were reduced in comparison with those of FW-wt rats (24.6% and 15.0%, respectively). The reduction of $CD4^+$ T cells was more pronounced than that of $CD8^+$ T cells. On the other hand, $CD4^+/CD8^+$ cells were few in FW-wt rats (3.0%) but markedly increased in number in FW-pX rats (21.0%). In FW-wt rats, $CD4^+$ cells were made up of $CD4^{medium}$ and $CD4^{high}$ populations. By contrast, the majority of $CD4^+/CD8^+$ cells in FW-pX rats expressed CD4 at a medium level. Jefferies et al[6] reported that rat $CD4^{medium}$ and $CD4^{high}$ populations represented monocytes and T cells, respectively, whereas Nascimbeni et al[20] showed that some $CD4^+/CD8^+$ T cells expressed CD4 at a medium level. Thus, we decided to examine whether $CD4^+/CD8^+$ cells in FW-pX rats were monocytes or T cells.

$CD4^+/CD8^+$ cells in the peripheral blood of FW-pX rats are monocytes

Peripheral blood was obtained from 6-week-old FW-pX rats. At first, we gated $CD4^+/CD8^+$ DP cells and confirmed that these cells

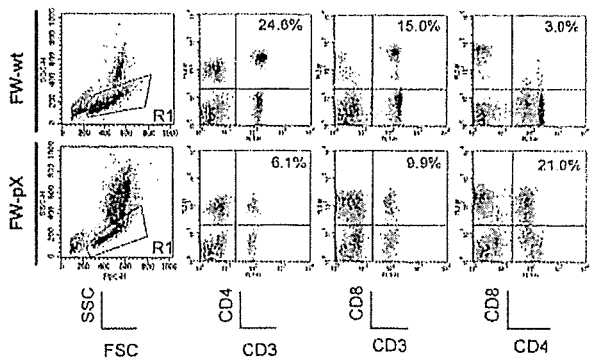

Figure 1. Expansion of $CD4^+/CD8^+$ cells in the peripheral blood of FW-pX rats. The top and bottom panels show the results of FCM analyses of peripheral blood from 6-week-old FW-wt (F1 generation of wild-type F344 and Wistar) and FW-pX (F1 generation of HTLV-I *pX* transgenic F344 and wild-type Wistar) rats, respectively. Peripheral blood cells were stained with FITC-conjugated anti-CD3 (G4.18), FITC- or PE-conjugated anti-CD4 (OX-35), and PE-conjugated anti-CD8 (OX-8) Abs, followed by depletion of erythrocytes. At first, the cells were divided based on the forward (FSC) and side scatter (SSC) patterns. Then, PBMCs in region 1 (R1) were gated to analyze the expression of CD3, CD4, and CD8. In both groups, at least 3 rats were examined. Representative data are shown. The numbers in each panel represent the percentage of $CD4^+$ T cells, $CD8^+$ T cells, and $CD4^+/CD8^+$ cells, respectively.

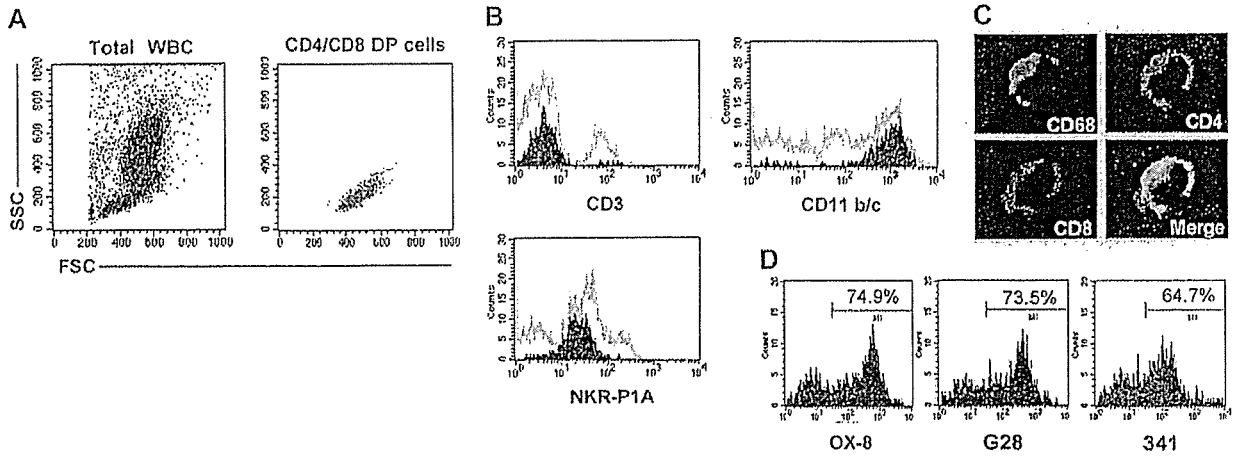

Figure 2. Characterization of CD4+/CD8+ cells in the peripheral blood of FW-pX rats. Peripheral blood from 6-week-old FW-pX rats was used. In each experiment, at least 3 rats were used. Representative data are shown. (A) Peripheral blood cells were stained with FITC-conjugated anti-CD4 (OX-35) and PE-conjugated anti-CD8 (OX-8) Abs, followed by depletion of erythrocytes. CD4/CD8 DP cells were gated to confirm that these cells were mononuclear cells. WBCs indicates white blood cells. (B) Peripheral blood cells were stained with FITC- or PE-conjugated anti-CD4 (OX-35), PerCP-conjugated anti-CD8 (OX-8), and FITC- or PE-conjugated anti-CD3 (G4.18), CD11b/c (OX-42), or NKR-P1A Ab (10/78), followed by depletion of erythrocytes. Painted histograms represent the expression of CD3, CD11b/c, and NKR-P1A on CD4+/CD8+ cells. Gray histograms represent the expression of these molecules on total PBMCs. (C) Mononuclear cells separated from the spleen of FW-pX rats were cultured in chamber slides at 37°C for 1 hour. Resultant adherent cells were fixed using cold acetone for 5 minutes and then stained for CD68 (ED-1, green), CD4 (OX-35, red), and CD8 (OX-8, blue). The merged image shows the cell stained with 3 colors (total magnification: × 600). (D) Peripheral blood cells were stained with FITC-conjugated anti-CD4 (OX-35) and PE-conjugated anti-CD8 Abs for the α-chain hinge region (OX-8), α-chain Ig V–like region (G28), or β-chain (341) followed by depletion of erythrocytes. Histograms represent reactivity with the anti-CD8 Abs gated on $CD4^{medium}$ cells.

were mononuclear but not aggregated cells (Figure 2A). Since rat monocytes could not be separated from lymphocytes or NK cells according to the light scatter pattern alone, we examined the expression of surface markers specific for each type of cell. Histograms were obtained by gating of $CD4^+/CD8^+$ cells (Figure 2B). Most $CD4^+/CD8^+$ cells in FW-pX rats were $CD11b/c^{high}$ and $NKR\text{-}P1A^{low}$ but did not express CD3. CD11b/c is expressed on monocytes, granulocytes, and macrophages, thereby known as a marker of myeloid cells.[21] NKR-P1A is highly expressed on NK cells and some T cells but expressed on monocytes at a low level.[22,23] We additionally found that the $CD4^+/CD8^+$ cells did not express OX-62, a marker for DCs[24] (data not shown). These observations suggest that these DP cells have a monocytic but not T, NK, or DC phenotype. To further confirm this suggestion, adherent splenocytes from 6-week-old FW-pX rats were stained for OX-35 (anti-CD4), OX-8 (anti-CD8), and ED-1 (anti-CD68, as a marker for monocytes/macrophages[25,26]) and then observed using a confocal microscope. The 3-color merged image indicates that the DP cells also express CD68 (Figure 2C). It is known that human CD68 can be expressed in activated T and B cells at a low level.[27,28] However, there was no $CD68^+$ population that expressed CD3 or the B-cell marker RLN-9D3 in our rat model. We therefore designated these $CD4^+/CD8^+$ cells as DP monocytes. In addition, we noted that CD4 and CD8 were distributed not only on the cell surface but also in the cytoplasm of DP monocytes. These findings are consistent with the previous observation that CD4 is also expressed in the cytoplasm of human monocytes.[29]

The majority of CD8 molecules are heterodimers composed of α- and β-chains. On the other hand, a subset of T cells and most NK cells are known to express CD8 as homodimers of α-chains.[30] Hirji et al[13] showed that rat alveolar and peritoneal macrophages express CD8 as αβ heterodimers but these CD8 molecules do not react with the anti-CD8 α-chain Ig V–like region Ab (G28). Since the anti-CD8 α-chain hinge region Ab (OX-8) can recognize macrophage CD8, these authors suggested that the Ig V–like region of the CD8 α-chain was masked or modified on rat alveolar and peritoneal macrophages. To analyze the subunit organization of CD8 molecules expressed on the DP monocytes, we performed 2-color FCM analysis using the anti-CD4 (OX-35) and 3 kinds of anti-CD8 Abs, including OX-8, G28, and anti–β-chain Abs (341). Histograms were obtained by gating of $CD4^{medium}$ cells in PBMCs isolated from 6-week-old FW-pX rats (Figure 2D). The percentage of cells reactive with OX-8 (74.9%) was comparable to that stained with G28 (73.5%). The CD8 β-chain was expressed in 64.7% of $CD4^{medium}$ cells. Thus, CD8 molecules expressed on the surface of DP monocytes in FW-pX rats are heterodimers composed of the β-chain and the α-chain with the conserved Ig V–like region.

Induction of DP monocytes in nontransgenic FW-wt rats

To examine whether DP monocytes are induced exclusively in FW-pX rats carrying the HTLV-I *pX* gene or also in other inflammatory situations unrelated to the transgene, we inoculated porcine myosin into the footpads of 3-week-old FW-wt rats along with the adjuvant containing killed tuberculosis germs. It is known that $CD4^+$ T cells down-regulate their surface CD4 under certain activating conditions.[31] However, we observed no significant down-regulation of CD4 molecules in T cells of our myosin-immunized rats (Figure 3A). The percentages of $CD3^+$ T cells in $CD4^{medium}$ cells were 5.9% and 5.5% in the FW-wt rats with and without immunization, respectively. Thus, we concluded that $CD4^{medium}$ cells were monocytes. One week after immunization, the percentage of $CD8^+$ population in $CD4^{medium}$ cells reached 57.3% ± 6.1% in myosin-immunized FW-wt rats, which was comparable to the proportion observed in 4-week-old FW-pX rats (63.5% ± 6.5%; Figure 3B-C). Four weeks after immunization, the percentage of $CD8^+$ population in $CD4^{medium}$ cells declined to 40.6% ± 7.3% in myosin-immunized FW-wt rats, whereas that in 7-week-old FW-pX rats was maintained at a high level (61.4% ± 4.8%). In 4- and 7-week-old FW-wt rats without immunization, the size of $CD8^+$ population in $CD4^{medium}$ cells was smaller (26.1% ± 14.6% and 23.5% ± 16.3%, respectively). These